A DISSERTATION FOR THE DEGREE OF DOCTOR OF PHILOSOPHY

Preparation and characterization of cellulose nanofibril aerogel cross-linked with maleic acid and sodium hypophosphite

말레인산과 차아인산나트륨을 이용한 가교 결합된 셀룰로오스 나노피브릴 에어로젤의 제조 및 특성 연구

Advisor Professor: Dr. Hak Lae Lee

By Chae Hoon Kim

PROGRAM IN ENVIRONMENTAL MATERIALS SCIENCE

DEPARTMENT OF FOREST SCIENCES

GRADUATED SCHOOL

SEOUL NATIONAL UNIVERSITY

February, 2015

Abstract

Preparation and characterization of cellulose nanofibril aerogel cross-linked with maleic acid and sodium hypophosphite

Chae Hoon Kim
Program in Environmental Materials Science
Department of Forest Sciences
Graduate School
Seoul National University

Cellulose nanofibril (CNF) is defined as a nano-scale fibrous material which can be obtained from cellulose fiber by means of a mechanical shearing action. Its diameter is in the range of 5 – 50 nm and its length is typically several micrometers. CNF is being studied by academia and industry for various applications; however, the most promising of these is considered to be as a starting material for the preparation of cellulose aerogel. An aqueous suspension of CNF produces a homogeneous hydrogel structure at a concentration of 1 wt % due to mechanical entanglement and interfibrillar hydrogen bonding. This unique capability of CNF to build up a self-assembled hydrogel structure allows for the preparation of a highly porous aerogel through direct water removal by means of freeze-drying. However, the network

structure of CNF aerogels is built by interfibrillar hydrogen bonds between adjacent individual fibers. As a result, the network structure of CNF aerogel is easily destroyed by absorbed water. This weakness of the wet strength limits the wider application of the CNF aerogel.

In this research, a cross-linked CNF aerogel was prepared. As cross-linking agents, maleic acid and hypophosphite were used. The cross-linking reaction was composed of esterification between maleic acid and cellulose in a suspension state and the formation of cross-linking by means of chemical bonds between cellulose-grafted maleic acid and hypophosphite in an aerogel state. Through this cross-linking reaction, the network stability of the CNF aerogel in a wet state was reinforced. Unlike typical CNF aerogels, the cross-linked CNF aerogel maintained its original shape after immersion in water under a mild shear condition. Moreover, the cross-linked CNF aerogel was rapidly able to absorb considerable amounts of water. The cross-linked CNF aerogel exhibited shape-recovery characteristics as well in a wet state. The shape-recovery characteristics of the wet cross-linked CNF aerogel were explained in terms of the interaction between the absorbed water and the amorphous region of the CNF.

As potential applications, carrying media or a supporting matrix for precious materials are feasible. In order to evaluate the potential applicability of these suggestions, the ion-adsorption performance of the cross-linked CNF aerogel was investigated. The surface charge of CNF was made positive by means of a surface modification with glycidyltrimethylammonium chloride (GTMAC). Through an etherification process, GTMAC was grafted onto the

surface of the CNF and the zeta potential of the cationic CNF was then increased to +39.5 mV. From the cationically modified CNF, a positively charged cross-linked CNF aerogel was prepared. The functional groups generating the surface charge of the positively charged cross-linked CNF aerogels were quaternary ammonium and carboxylic groups. For the negatively charged cross-linked CNF aerogel, only carboxyl groups contributed to the surface charge. As a result, the zeta potential of both cross-linked CNF aerogels was affected by the pH of the aqueous media. The pH also affected the ion-adsorption performance of the cross-linked CNF aerogels. An adsorption isotherm was carried out and the theoretical maximum adsorption performances of the cross-linked CNF aerogels were calculated using the Langmuir adsorption model. The n_s value, representing the maximum ion-absorption capacity of the negatively charged cross-linked CNF aerogel, was 0.79 mmol/g for nickel ion, while the n_s value of the positively charged aerogel was 0.62 mmol/g for permanganate ions. These values are low relative to previously reported performance levels of chemically modified micro-particular cellulose absorbent materials, but they are higher than those of commercially available strong acid ion-exchange resins.

Keywords: cellulose nanofibril, aerogel, cross-linking, shape recovery, cationic modification, ion adsorption

Student number: 2008-21294

Contents

List of Tables

List of Figures

Chapter 1

Introduction

1. Introduction

Cellulose is the most abundant and renewable biopolymer which can be derived from biomass on earth. Its annual production is estimated to be 1010 – 1011 tons (Samir et al. 2005). By far, woody biomass is the source of most cellulose. Cellulose is a fibrous, water-insoluble polymer with excellent mechanical properties, lending structural support to trees through the production and utilization of cellulose as the main structural material. Additionally, non-woody plant fibers (e.g., cotton, hemp, kenaf), algae, fungi, bacteria, and marine animals (tunicate) are also important sources of cellulose.

A highly developed hierarchical structure is the most important characteristics of cellulose fiber. Cellulose is a homopolysaccharide which consists of a linear chain of β(1→4)-linked anhydro-D-glucose units. Monomeric glucose includes three hydroxyl groups, which contribute to the formation of the fiber structure. During biosynthesis, van der Waals forces and inter- and intramolecular hydrogen bonds are developed between adjacent hydroxyl groups. As a result, cellulose chains are aggregated in elemental fibrils with a diameter of 2 – 20 nm. These cellulose microfibrils are aggregated into a fiber bundle by interfibrillar hydrogen bonds, thus composing the fiber.

Cellulose nanofibril (CNF) is defined as a nano-scale fibrous material which can be obtained from cellulose fiber by means of a mechanical shearing action. CNF is composed of an aggregation of 10 – 50 cellulose elemental fibrils. Its diameter ranges from 5 to 50 nm and it length is typically several micrometers.

Given its high specific surface area and strong mechanical properties, CNF has been studied by academia and industry for various applications. For example, CNF has been employed as a reinforcing agent for biocomposite materials (Shibata et al. 2010) or as a building material for translucent sheets (Yano et al. 2005). However, one of the most promising applications is considered to be as a starting materials for the preparation of cellulose aerogels.

Aerogels are high porous, ultra-lightweight materials that are formed by the removal of the liquid dispersion medium from the gel without a collapse of the network structure (Hüsing et al. 1998). Since the introduction of aerogels by Kistler (1931), they have commonly been prepared by a sol-gel process and the supercritical fluid drying of inorganic metal-oxide materials or polymers (Pierre et al. 2002). However, these processes require multiple solvent-exchange stages and considerable amount of energy as well. Therefore, there are environmental and economic issues which need to be solved.

CNF is a long and flexible nanofiber with an aspect ratio greater than 1000. As a result, CNF produces a homogeneous hydrogel structure in an aqueous suspension due to mechanical entanglement at a concentration 1 wt %. This unique ability of CNF to build up a self-assembled hydrogel structure allows for the preparation of highly porous aerogels through direct water removal by means of freeze-drying (Pääkkö et al. 2008). Furthermore, numerous hydroxyl groups exist on the CNF surface due to its intrinsic chemical structure, and dried CNF produces strong interfiber hydrogen bonds. Indeed, there is no need for any crosslinking treatment when using the sol-gel process and solvent exchange method, nor is supercritical drying needed, unlike conventional aerogels.

Besides the high porous structure and high specific surface area, the CNF aerogel exhibits flexible mechanical characteristics, unlike most aerogels, which are brittle. Furthermore, various functionalities can be instilled into CNF aerogels for different applications through the use of the numerous hydroxyl groups as a starting point for a chemical modification process. Therefore, many potential applications can be expected when using CNF aerogels, such as kinetic energy absorbers, thermal and acoustic insulating materials, reinforcing platforms, and drug carrier and tissue engineering scaffolds (Sehaqui et al. 2010).

However, the network structure of CNF aerogel is built by interfibril hydrogen bond. In high humidity or wet condition, interfibril bond of CNF aerogel is weaken by water molecule therefore aerogel network is easily destroyed. This weakness of wet strength limits the wide application of CNF aerogel.

2. Objectives of the study

CNF is an attractive material for the production of aerogels. Without an additional treatment, CNF in aqueous suspension easily builds up a hydrogel with a three-dimensional fiber network structure because of its morphological and surface chemical properties. During the freeze-drying of CNF hydrogel, porous fiber network is maintained and strong interfibril bond is formed by hydrogen bond because of abundant hydroxyl groups of cellulose. Therefore, a highly porous and ultralight aerogel with strong mechanical properties is produced. However, interfibril hydrogen bond becomes a major disadvantage of CNF aerogel when exposed to aqueous condition. In high humidity or wet condition, CNF aerogel is severely weaken and easily destroyed.

The main objective of this study is to improve the network stability of CNF aerogel in wet state by means of the covalent cross-linking treatment of cellulose. Physical, mechanical, and structural characteristics of prepared cross-linked CNF aerogel were investigated. As a method for imparting additional functionalities for a wider range of potential applications of the cross-linked CNF aerogel in aqueous media, the surface charge characteristics of the CNF aerogel was modified and its adsorption performance was investigated.

3. Literature reviews

3.1. Mechanical treatments for the preparation of CNF

The preparation of a nano-scaled cellulose fibrous material through a mechanical treatment was reported for the first time by Turbak et al. (1983) and by Herrick et al. (1983). They successfully isolated cellulose microfibrils from cut cellulose fiber using a Gaulin laboratory homogenizer. During the homogenizing process, cellulose fiber slurry is pumped toward the valve assembly under a high pressure. As the fiber passes through the fine gaps of the valve, the pressure is drastically decreased and the fiber is therefore subjected to high shearing forces. Although they reported this mechanical treatment process nearly 30 years ago, this concept is still widely used by many researchers (Nakagaito et al. 2004, Iwamoto et al. 2005, Aulin et al. 2009).

Another mechanical treatment for the preparation of CNF involves the use of a microfluidizer. Inside the microfluidizer, cellulose fiber is passed through a z-shaped microchannel at a high pressure, up to 2070 bar. As a result, the cellulose fiber encounters a high shear rate up to 10^7 s^{-1} and is disintegrated into CNF (Siqueira et al. 2010).

A grinder can also be used to treat cellulose fiber mechanically (Taniguchi et al. 1988, Iwamoto et al. 2007). As the pulp slurry is passed through a gap between a static grinding stone and a rotating grinding stone, shear force is applied and cellulose nanofibers are produced as a result.

In addition to the mechanical treatment methods above, other techniques such as cryo-crushing (Dufresne et al. 1997, Chakraborty et al. 2005, Alemdar et al. 2008), the use of refiners (Heiskanen et al. 2012), or the use of a high-speed blender (Uetani and Yano 2011) have also been employed.

3.2. Pretreatments for the preparation of CNF

To produce CNF by means of the mechanical disintegration of cellulose fibers into a nano-scale fibrous material, much energy is inevitably consumed. It was reported that during the high-pressure homogenization process of creating CNF, a maximum energy of 70,000 kWh/t can be consumed (Eriksen et al. 2008). Zimmermann et al. (2010) also evaluated the energy used by the microfluidizer process. As the pass numbers were increased, the viscosity of the fiber slurry and the energy consumption both increased sharply. For example, only 8.5 kW was required for four passes, whereas 14,875 kW was needed for seven passes. High energy consumption during the process of its production is one of the main drawbacks of CNF; therefore, several pretreatment techniques have been developed.

The most promising pretreatment technique is an oxidation process mediated by 2,2,6,6-tetramethyl-piperidine (TEMPO) which modifies the cellulose surface under a mild aqueous condition (Saito and Isogai 2004, Saito et al. 2006, 2007, Isogai et al. 2011a). TEMPO-mediated oxidation involves the oxidation of cellulose through the addition of NaClO into the cellulose fiber suspension with TEMPO as a catalyst and NaBr at pH 10-11 at room temperature. By means of the catalytic reaction of TEMPO, the primary hydroxyl groups of cellulose are selectively oxidized to a carboxylate group, and only NaClO and NaOH are consumed. As a result, the interfibrillar hydrogen bonding between the adjacent cellulose microfibril is inhibited by the electrostatic repulsion force induced from the carboxylic acid, thus facilitating the disintegration of the cellulose nanofibril. Based on the same principle,

several modified TEMPO-mediated oxidation pretreatment methods have been reported. Hirota et al. (2009) and Saito et al. (2009) employed a modified TEMPO-mediated oxidation system that uses $NaClO_2$ as the main oxidant and NaClO instead of NaBr. This system is effective under a more mild condition, pH 7. Another system, a TEMPO electro-mediated oxidation system, was reported by Isogai et al. (2011a) and Isogai et al. (2011b). In this system, oxidation is carried out with 4-acetamido-TEMPO at pH 6.8 without NaClO or $NaClO_2$. Compared to the two oxidation systems above, a similar level of carboxylate content is achieved in this case, although longer oxidation times are required.

After the TEMPO-oxidation pretreatment, the interfibrillar hydrogen bonding of the cellulose microfibril is inhibited; therefore, a low intensity of the shear force is required for the full disintegration of the CNF. Typically, a blender or a homogenizer is employed for a mechanical treatment; however, Johnson et al. (2008) reported that 97.5 % of CNF recovery can be achieved by ultrasonication for 30 min. When the ultrasonication time was increased to 4 hours, CNF with a thickness of 0.74 nm was produced.

In terms of energy consumption, Isogai et al. (2011) reported that with a TEMPO-mediated oxidation pretreatment, energy consumption could be reduced considerably. Compared to the energy consumption of 1400 MJ/kg for the high-pressure homogenizer process of untreated slurry, only 7 MJ/kg was required when TEMPO-oxidation was applied before the homogenizer process.

Energy consumption during the CNF mechanical process can be reduced through an enzymatic pretreatment of cellulose fiber. With the enzymatic

hydrolysis of fiber, cellulose is slightly degraded by cellulase. Specifically, an amorphous region of cellulose is selectively hydrolyzed due to its higher accessibility to enzymes. As a result, the disintegration of cellulose microfibril is facilitated (Pääkkö et al. 2007). Henriksson et al. (2007) also reported that with an enzymatic pretreatment, the endoglucanase swelling of pulp fiber was increased, thus facilitating the disintegration of the fiber during a high-pressure homogenization process. Siqueira et al. (2010a, 2010b) focused on the impact of enzymatic pre- and post-treatments on the morphology of CNF and on the final properties of a CNF-rubber composite. One notable finding was that the results were highly dependent on a combination of endoglucanase and an exoglucanase treatment conditions during the pre- and post-treatments.

Another pretreatment system is carboxymethylation (Aulin et al. 2010). With a principle similar to that of the TEMPO-mediated oxidation system, carboxy-methylation increases the anionic charge of the cellulose microfibril. This results in low energy consumption during the mechanical disintegration process. Taipale et al. (2010) reported that after a carboxymethylation pretreatment, the specific energy consumption of the microfluidizer was 2.2 MWh/t, while 5.5 MWh/t was needed when a pretreatment was not used.

3.3. Surface modification of cellulose nanomaterials

On account of the abundant hydroxyl groups of the cellulose backbone chain, CNF is a hydrophilic material which is not compatible with non-polar polymer matrixes or solvents. When mixed with non-polar media, CNF forms irreversible aggregation or surface passivation so as to reach an energetically favorable state (Johansson et al. 2011). Through a surface modification technique, this limitation of the commercial application of CNF can be overcome. Moreover, various new functionalities can be realized, and the range of potential applications of CNF can be widened through the surface modification approach.

Surface modifications of CNF include surface adsorption, molecule grafting, and polymer grafting (Missoum et al. 2013). The surface properties of CNF can be tuned by the physical adsorption of chemicals with different desired functionalities. The most common materials are surfactants. Syverud et al. (2011) treated CNF with a surfactant in an effort to improve its compatibility with non-polar media. On the surface of CNF films, *n*-hexadecyl trimethyl-ammonium bromide (cetyltrimethylammonium bromide, CTAB) was adsorbed and the hydrophilic characteristics of the CNF film changed, becoming more hydrophobic, without a change of the mechanical properties. Xhanari et al. (2011) also reported a similar result using surfactants with different chain lengths (cetyltrimethyl-, didodecyl-, and dihexadecyl ammonium bromide.) Ryu et al. (2012) adjusted the CNF network characteristics by means of polymer adsorption. As polyethylenimine was adsorbed onto the CNF surface, the aggregation of CNF occurred and the network strength and dehydration

speed increased as a result. A layer-by-layer (LbL) technique was also employed as a means of the surface modification of CNF. Wägberg et al. (2008) built up polyelectrolyte multilayers (PEM) on the CNF surface with poly(dimethyl diallyl ammonium chloride), polyethylenimine, and poly(allylamine hydrochloride). As the polyelectrolyte layers were deposited on the CNF surface, the surface charge of the CNF alternated between a positive and a negative charge, and the thickness of the PEM increased.

By the molecule grafting, chemicals with various functional groups can be introduced onto the CNF surface; consequently, surface properties of CNF can be modified. Due to the abundant hydroxyl groups on the surface of CNF, different graft reactions such as etherification, esterification, oxidation, sialylation, or acetylation can be employed (Habibi et al. 2010). The surface charge property of CNF was modified through an etherification process. Ho et al. (2011) treated cellulose nanocrystal with chlorocholine chloride (ClChCl) in DMSO media. They reported that cationically modified CNF produced more transparent films than non-modified CNF and that clay was dispersed better in a cationic CNF suspension. Jin et al. (2011) reported that cationically modified nanocellulose film exhibited antibacterial activity toward both Gram-positive and Gram-negative bacteria. During the application of CNF as a biocomposite, miscibility with the polymer matrix is the most pertinent issue. Therefore, various surface modifications for hydrophobicity have been studied. Rodionova et al. (2010) reported the gas-phase surface esterification of CNF with trifluoroacetic acid anhydride and acetic acid in an effort to prepare hydrophobic CNF films. In research by Tingaut et al. (2010), acetylation was employed to prepare hydrophobic CNF. The grafting of acetyl moieties not only

prevented the hornification of CNF during the drying process but also improved the dispersibility of CNF in chloroform. As a result, the degree of miscibility with poly(lactic acid) was increased and the biocomposite showed improved filler dispersion capabilities, greater thermal stability, and reduced hygroscopicity. Likewise, in the research of Jonoobi et al. (2010) kenaf fibers were acetylated and then mechanically disintegrated. The resulting hydrophobic kenaf fibers were more easily isolated compared to non-treated fibers. Goussé et al. (2004), Andresen et al. (2007), and Lu et al. (2008) reported the sialylation of CNF. The hydrophobic CNF exhibited good performance as a water-in-oil emulsion stabilizer (Andresen et al. 2007). In research by Lu et al. (2007), CNF was treated with 3-aminopropyl-triethoxysilane, 3-glycidoxypropyl-trimethoxysilane, and a titanate coupling agent. The resulting hydrophobic CNF and an epoxy resin composite showed improved mechanical properties, with good adhesion between the CNF fibers and the epoxy resin as well.

Polymer grafting onto the surface of CNF can be accomplished by means of two methods: the “grafting-onto” and the “grafting-from” methods (Zhao and Brittain 2000). In the “grafting-onto” approach, presynthesized polymer chains are attached onto the hydroxyl groups of the cellulose using a coupling agent. Therefore, the molecular weight of the attached polymer can be easily controlled. However, the grafting yield is relatively low due to the steric hindrance induced by the attached polymer chains.

In the “grafting-from” approach, initiators are immobilized onto the CNF surface and polymers are in-situ polymerized using an initiator. Therefore, a

higher graft yield becomes feasible due to the lower steric hindrance compared to the “grafting-onto” approach. However, a homopolymer also forms during the polymerization process, and it is difficult to inhibit this.

The “grafting-from” approach was employed by Li et al. (2011). In their research, CNF modified by 2-bromoisobutryl was prepared. The grafted functional groups were activated, and poly(butyl acrylate)(PBA) was synthesized in situ by means of atom-transfer radical polymerization. The PBA-grafted CNF was mixed with polypropylene and the resulting biocomposite exhibited significantly improved compatibility, interface adhesion, and mechanical strength with an increase in the degree of polymerization of the PBA chain. Littunen et al. (2011) prepared a CNF composite using a redox-initiated free radical method. Cerium ammonium nitrate was used as an initiator and the polymer in their study was synthesized using the acrylic monomers of glycidyl methacrylate, ethyl acrylate, methyl methacrylate, butyl acrylate, and 2-hydroxyethyl methacrylate. The nanofibrillar morphology of CNF was not changed by the polymerization process and the resulting hydrophobic polymer-grafted CNF exhibited improved heat resistance. In research by Lönnberg et al. (2011), CNF was grafted with poly(lactic acid) via ring-opening polymerization. Biocomposite materials containing 0, 3, and 10 wt % CNF were prepared, and the strongest biocomposite materials were obtained after reinforcement with CNF grafted with the longest poly(lactic acid) graft chain.

3.4. Preparation of cellulose aerogel

Cellulose aerogels can be prepared with either dissolved cellulose or aqueous cellulose nanofibers according to the type of cellulose starting material.

3.4.1. Cellulose aerogel made by dissolving cellulose

Owing to its strong intra- and inter-molecular hydrogen bonds, cellulose cannot be dissolved in most solvents. Nonetheless, several solvent systems are able to dissolve cellulose. Cellulose can be dissolved in alkali solutions such as LiOH and NaOH, though it must be pretreated. Several organic solvents, such as N-methylmorpholine-N-oxide (NMMO), N,N-dimethylacetamide (DMAc), dimethylsulfoxide (DMSO), and N-N-dimethylimidazolidinone (DMI), are widely employed to dissolve cellulose (Isogai and Atala 1998, Wang et al. 2008) as well.

In the research of Qi et al. (2013), cellulose was dissolved in a NaOH/urea solution. A NaOH/urea solution containing multi-walled carbon nanotubes (MWCNTs) was precooled to -120 ℃. Cotton linters were added to the mixture, and after vigorous stirring for 5 minutes, a cellulose-MWCNT solution was produced. A sol-gel step was then carried out by immersing the cellulose solution into an H_2SO_4 solution for 5 minutes. After the rapid freezing and freeze-drying of the hydrogel, a cellulose-MWCNT nanocomposite aerogel was produced. Likewise, systems of LiCl/DMAc and of LiCl/DMSO for dissolving cellulose to produce cellulose aerogel were employed by Duchemin et al. (2010) and by Wang et al. (2012), respectively.

A supercritical CO_2 drying process is widely used to prepare inorganic aerogel with silica, carbon nanofiber, or clay, among other materials. This drying technique has also been utilized to prepare cellulose aerogels. Tan et al. (2001) prepared a cellulose aerogel using cellulose acetate and cellulose acetate butyrate as starting materials. These cellulose esters were dissolved in acetone and cross-link-treated with diisocyanate. Then, gelation took place in a mechanical shaker for 1 – 15 days. The resulting cellulose gel was exposed to supercritical CO_2 at a pressure of 5.3 MPa and at a temperature of 4 ℃ for 5 days, followed by 11.7 MPa and 50 ℃ for 6 hours. The pressure was subsequently decreased gradually to atmospheric pressure at 50 ℃. The resulting cellulose aerogel showed high mechanical strength. Liebner et al. (2008), Gavillon et al. (2008), and Cai et al. (2012) also reported cellulose aerogels prepared by the supercritical CO_2 drying of dissolved cellulose gel; however, different methods for preparing the dissolving cellulose were applied. Liebner et al. (2008) dissolved cellulose in *N*-methylmorpholine -*N*-oxide (NMMO) at 100 ℃. Gelation was then carried out by the cooling of molten NMMO containing cellulose. In research by Gavillon et al. (2008), microcrystalline cellulose was dissolved in a NaOH/water solution. Gelation was done by increasing the temperature of the cellulose/NaOH/water solution. After supercritical CO_2 drying, highly porous cellulose aerogel with a specific surface area as large as 280 m^2/g of was produced. Cai et al. (2012) produced a cellulose-silica nanocomposite aerogel by dissolving cellulose in a LiOH/urea solution.

3.4.2. Cellulose aerogel made from aqueous cellulose nanofibers

For the first time, Pääkkö et al. (2008) prepared a cellulose aerogel by means of the freeze-drying of CNF hydrogel. CNF is a nano-sized flexible fibrous material which can be used easily to build a complex three-dimensional fiber network structure by mechanical entanglement in aqueous media. As a result, the CNF suspension forms a hydrogel structure at a very low concentration above 1 wt%. During a freeze-drying process, the volume of the CNF suspension is maintained without a collapse of the three-dimensional fiber network, and CNF aerogel is produced. Also, after freeze-drying, hydroxyl bonds are formed between adjacent cellulose nanofibrils. Thus, the CNF aerogels exhibit strong mechanical properties.

Aulin et al. (2010) also prepared a cellulose aerogel by the freeze-drying of a CNF suspension. CNF was produced by a high-pressure homogenizer treatment of pulp dissolved by a carboxymethyl treatment. After rapid freezing in liquid nitrogen followed by freeze-drying, the CNF aerogel was produced. The density of the aerogel was almost linearly proportional to the CNF suspension concentration. Sehaqui et al. (2010) also prepared a cellulose aerogel using a similar process; however, they added xyloglucan (XG) to the CNF suspension as a mechanical strength enhancer. The resulting cellulose-XG aerogel exhibited greater mechanical strength compared to conventional polymer/silica aerogels. Cervin et al. (2012), Chen et al. (2011), and Zhang et al. (2012) also prepared cellulose aerogels rapid by the freezing and the freeze-drying of CNF suspensions.

The supercritical fluid drying technique was also employed as drying

process for a cellulose nanofiber suspension. Heath and Thielemans (2010) used cellulose nanocrystal (CNC) as a starting material. They prepared cellulose hydrogel through the high-intensity ultrasonication of a CNC suspension. The hydrogel was then subjected to ethanol solvent exchange and a subsequent supercritical CO_2 drying step. Bacteria cellulose was also employed as a starting material for cellulose aerogels. Liebner et al. (2010) and Russler et al. (2012) produced bacterial cellulose using *Gluconacetobacter xylinum*. After 30 days of cultivation, bacterial cellulose layers with thicknesses of 3 – 4 cm were produced. These bacterial cellulose hydrogels underwent an ethanol solvent exchange treatment, and the resulting alcogels were subjected to supercritical CO_2 drying. The prepared bacterial cellulose aerogel exhibited an ultra-lightweight characteristic, and its density was only 8.25 mg/cm^3.

3.5. Functionalization of cellulose aerogel

CNF aerogels are fascinating materials with high porosity and a high specific surface area. The inherent high modulus and strength of the native cellulose and its biodegradability, biocompatibility, availability, renewability, and capacity for chemical modification are also important advantages of cellulose aerogels (Syverud and Stenius 2009, Yano et al. 2004). Therefore, cellulose aerogels have great potential applicability in various areas, such as kinetic energy absorbers, thermal and acoustic insulators, in pharmaceutical and biomedical applications as drug carrier and tissue engineering scaffolds, and as storage materials (Sehaqui et al. 2010).

CNF aerogels can be chemically functionalized in various ways with different applications. The most common approach is a hydrophobic treatment for the application of the CNF aerogel as an oil absorbent. Jin et al. (2011) treated CNF aerogels with (tridecafluoro-1,1,2,2,tetrahydroocyl)trichlorosilane (FTCS) using a chemical vapor deposition (CVD) technique. After a post-treatment, the prepared superhydrophobic CNF aerogel exhibited excellent oil-absorbing performance. Similarly, Cerving et al. (2012) and Zheng et al. (2014) also prepared an oil-absorbing CNF aerogel by the CVD of silane chemicals. As an alternative to the silane treatment, Korhonen et al. (2011) reported that a superhydrophobic CNF aerogel can be prepared by means of TiO_2 nanoparticle deposition. In research by Kettinene et al. (2011), the wettability of a TiO_2-deposited CNF aerogel was controlled by exposure to UV light. However, an oleophobic CNF aerogel was also prepared by the CVD of a fluorine chemical (1,1,2,2,-perfluorodecyltrichlorosilane) by Aulin et al. (2010)

The nanofibrillar network structure of CNF aerogels is easily destroyed by absorbed water; however, a potential application which replaces the superabsorbent polymer has been reported, demonstrating improved mechanical stability in a wet state. Brodin et al. (2012) prepared TEMPO-oxidized CNF and chemi-thermomechanical pulp (CTMP) composite aerogels. The CTMP fibers exhibited a mechanical reinforcing effect. Therefore, water adsorption capacity was nearly identical to that of a conventional superabsorbent polymer. Zhang et al. (2012) treated a CNF aerogel with polyamide-epichlorohydrin resin. The resulting cross-linked aerogel showed good network stability in water and good water absorbency.

In the research of Pääkkö et al. (2008), a CNF aerogel underwent a polyaniline-dodecyl benzene sulfonic acid (PANI(DBSA)) treatment. By dipping the CNF aerogel into a PANI(DBSA)-doped toluene solution, a PANI-functionalized aerogel with some conductivity was prepared. Similarly, Olsson et al. (2010) reported a CNF aerogel treated with cobalt ferrite nanoparticles which showed magnetic behavior. Koga et al. (2012) suggested that the CNF aerogel can be used as a catalyst template. They prepared a Cu(I) ion-adopted TEMPO-oxidized CNF aerogel through an ion-exchange process. The Cu-CNF aerogel exhibited excellent catalytic performance in an azide-alkyne Huisgen [3+2] cycloaddition reaction.

Chapter 2

Preparation of cross-linked cellulose nanofibril aerogel

1. Introduction

CNF is a long and flexible nanofiber with a high aspect ratio. In assessments of the morphological characteristics, CNF fibers become mechanically entangled in aqueous suspensions, and a homogenous hydrogel structure forms at a concentration of 1 wt %. After rapid freezing and freeze drying of CNF hydrogel, a highly porous and ultra-lightweight aerogel can be prepared. On the other hand, a conventional aerogel is prepared by a sol-gel process and with the supercritical fluid drying of inorganic materials or regenerated cellulose. Compared to the conventional aerogel, the CNF aerogel does not require multiple solvent-exchange or intensive energy-consuming drying processes.

In addition to the eco-friendly preparation process, various functionalities can be instilled into the CNF aerogel given its chemical structure and the hydroxyl groups of the cellulose used to create it. For example, superhydrophobic (Cerving et al. 2012), electroconducting (Pääkkö et al. 2008) and magnetic (Olsson et al. 2010) aerogels have been reported. Moreover numerous potential applications are expected, such as kinetic energy absorbers, thermal and acoustic insulating materials, reinforcing platforms, and drug carrier and tissue engineering scaffolds (Sehaqui et al. 2010).

However, the network structure of the CNF aerogel is built by the interfibrillar hydrogen bonding of adjacent fibers. When CNF is exposed to moisture, its hydrogen bonds weaken, causing the CNF aerogel to be destroyed easily. In this chapter, a cross-linked CNF aerogel was prepared using maleic acid and sodium hypophosphite. Maleic acid was grafted onto cellulose fiber,

with the covalent cross-linking of cellulose fibers formed by the ensuing reaction between the maleic acid and the sodium hypophosphite. The prepared cross-linked CNF aerogel exhibited improved network stability in a wet state, as well as good water absorbency. In addition, the physical, mechanical, and structural characteristics of the cross-linked CNF aerogel were investigated.

2. Materials and methods

2.1. Preparation of cellulose nanofibril

Commercial bleached eucalyptus kraft pulp was used as a raw material. Dried pulp sheets were dispersed in deionized water and were refined using a laboratory valley beater as a mechanical pretreatment. After 10 minutes of disintegration, the pulp slurry was beaten for 12 minutes and 30 seconds to obtain a freeness value of 450 mL CSF. The beaten pulp slurry was concentrated until its solids content was 2 wt %. The beaten fiber suspension was processed using a grinder (Super Masscollider MKCA6-3, Masuko Sanguo Co.). The pulp fibers were then passed through a gap between a static ceramic grinding stone and a rotating grinding stone revolving at 1,500 rpm. The gap was adjusted to -60 μm, with 40 passes.

After the grinding treatment, the viscosity of the fiber suspension was drastically increased and CNF suspension exhibited the properties of a hydrogel, as shown in Fig. 2-2. As shown in Fig. 2-3, the pulp fiber was separated into nanofibrils with widths ranging from 10 to 50 nm.

The chemical composition of the CNF produced was measured by the NREL (National Renewable Energy Laboratory, USA) method (NREL/TP-510-42618). The contents of α-cellulose, hemicellulose, lignin and ash were found to be 79.4%, 18.7%, 1.5%, and 0.5%, respectively.

It was reported that during the production of CNF, the cellulose chain is damaged and the degree of the polymerization of cellulose was diminished by mechanical shearing action (Abdul Khalil et al. 2014). The CED viscosity

levels of the pulp raw material, beaten pulp, and the produced CNF were measured according to the TAPPI T 230 om-99 method. The intrinsic viscosity and degree of polymerization were calculated from the measured viscosity according to a method devised by Shin (2011). This is listed in Table 2-1.

Table 2-1. CED viscosity and degree of polymerization of cellulose of untreated pulp, beaten pulp and CNF.

Sample	Viscosity (cPs)	DP
Untreated eucalyptus pulp	14.1 ± 0.4	1128 ± 20
Beaten pulp	13.8 ± 0.5	1113 ± 24
CNF	9.9 ± 0.6	891 ± 42

Fig. 2-1. Picture of a grinder and grinding stone

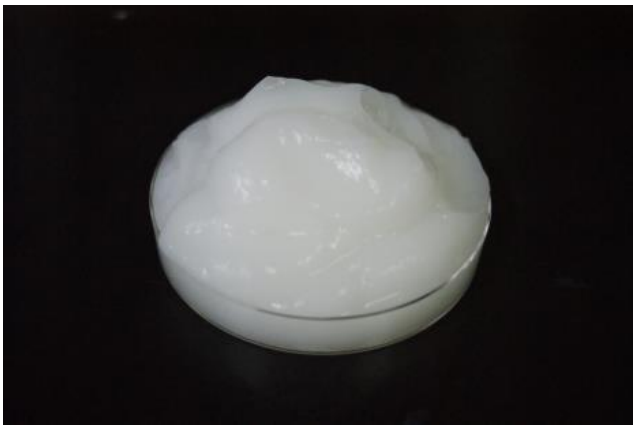

Fig. 2-2. Picture of CNF hydrogel

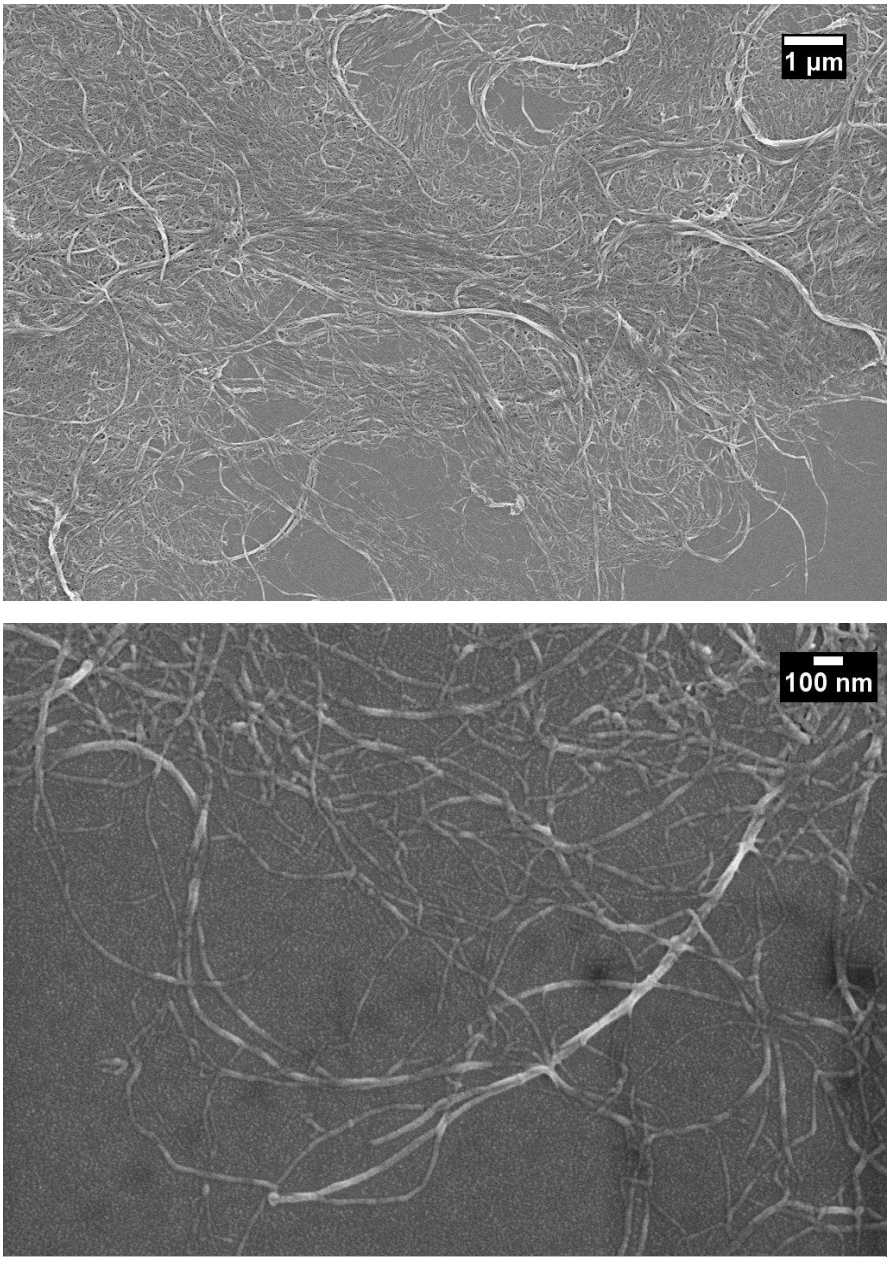

Fig.2-3. SEM images of prepared CNF

2.2. Preparation of cross-linked CNF aerogel

2.2.1. Esterification of CNF with maleic acid

For the cross-linking of the CNF aerogel, maleic acid and sodium hypophosphite were used as cross-linking agents. These reagent-grade chemicals were supplied by Sigma-Aldrich and were used as a 40 wt % aqueous solution without a further purification process.

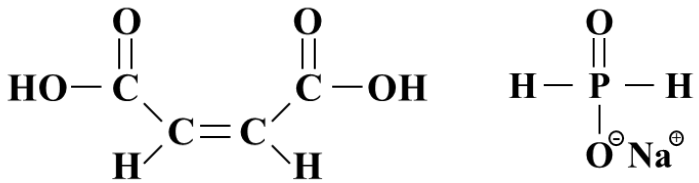

Fig. 2-4. Molecular structure of maleic acid (left) and sodium hypophosphite (right)

In this research, CNF was made from bleached hardwood kraft pulp. Therefore, it contains 18.7% of hemicellulose. However, it was assumed that the CNF consisted of only cellulose to simplify the estimation of the maleic acid dosage. The added amount of maleic acid was calculated as the molar ratio to the anhydroglucose unit (AGU) of cellulose, as follows: 0.1 to 10 moles of maleic acid per one mole of AGU. The amount of sodium hypophosphite was 10 wt% that of the maleic acid.

After mixing for 30 min, the CNF suspension containing maleic acid and hypophosphite was held at 120 ℃ for 30 min using an autoclave (MLS-3020, Sanyo Electric Co., Ltd.) for esterification between the maleic acid and cellulose. The maleic-acid-treated CNF (CNF-MA) suspension was centrifuged at 3,000 G for 10 min. After centrifuging, The CNFs were allowed to settle and clear supernatants were removed. The CNF-MA pad was re-dispersed in deionized water and additional centrifugal washing was carried out.

2.2.2. Preparation of CNF aerogel by freeze-drying of CNF hydrogel

After the centrifugal washing process, sodium hypophosphite was added to the CNF-MA suspension at an amount of 10 - 40 wt % based on the oven-dried CNF-MA. Next, the total solids content of the suspension was adjusted to 1.0 – 3.0 wt %, and it was transferred to a polystyrene cuvette as a mold. Before the rapid freezing process, the CNF hydrogels in the cuvette were placed in a refrigerator at 4 ℃ overnight. Through this precooling step, fracturing of the frozen CNF suspension during the rapid freezing process could be minimized (Zheng et al. 2014). The precooled CNF hydrogels were rapidly frozen at -196 ℃ using liquid nitrogen, and the frozen samples were subjected to freeze-drying using a freeze-dryer (FD8518, Ilshin Lab) for three days. The cold trap temperature was -80 ℃ and the vacuum level was maintained at 5 mmHg during the freeze-drying process. After three days of freeze-drying, rectangular CNF aerogels were prepared. The size of the CNF aerogel was 10 mm × 10 mm × 41.5 mm, corresponding to the volume of the cuvette mold.

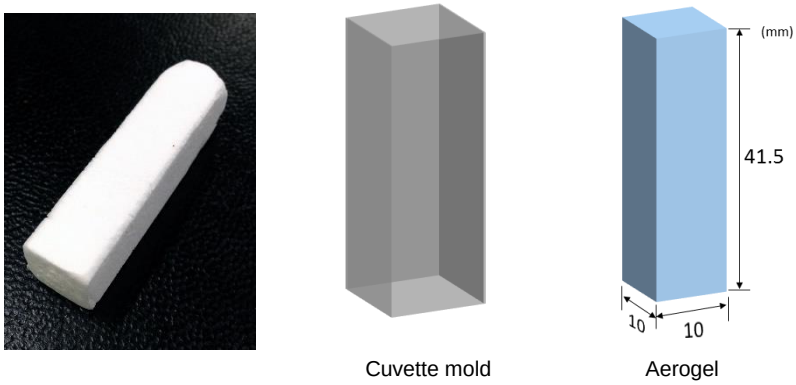

Fig. 2-5. Picture of produced cross-linked CNF aerogel and its dimensions

2.2.3. Formation of cellulose cross-linking

The CNF aerogels were cured in a convection oven to form cross-linking between the cellulose fibrils. The curing temperature was adjusted from 120 to 170 ℃ and the time was 10 min. At the temperature of 170 ℃, the curing time was varied from 1 to 30 min. After curing, no morphological changes of the CNF aerogel were observed. The resulting cross-linked CNF aerogels were cut into cubes 10 mm × 10 mm × 10 mm in size and were stored in a room with a controlled constant temperature and humidity (23 ℃ and 50 % RH) for further characterization.

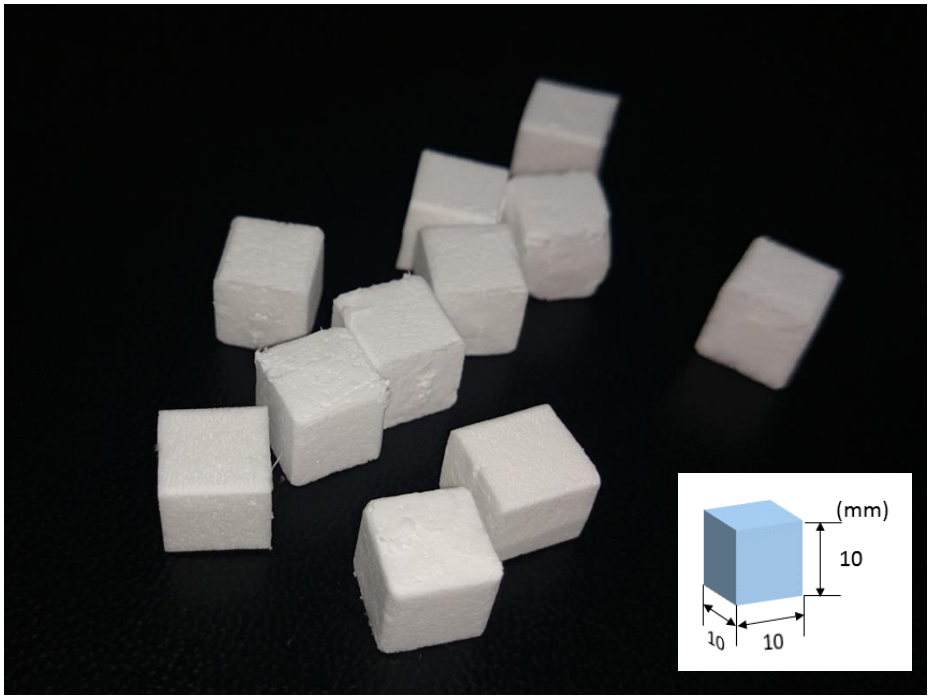

Fig. 2-6. Picture of prepared cubic shaped cross-linked CNF aerogel

2.3. Characterization of cross-linked CNF aerogel

2.3.1. FT-IR spectroscopy

FT-IR spectroscopy was utilized to identify the ester linkage between the maleic acid and the CNF. After the esterification process, the CNF-MA suspensions were treated with a 0.1 M NaOH solution at room temperature for 1 hour to convert carboxylic acid to carboxylate anion. The NaOH-treated CNF-MA suspension was vacuum-filtered and the resultant CNF-MA films were dried in a convection oven at 40 ℃ for 2 days. The FT-IR spectra were acquired from the CNF-MA films using a FT-IR spectrometer (Cary 660, Agilent) in ATR mode. For each spectrum, 32 scans were collected with a range of 600 - 4000 cm^{-1} at a resolution of 4 cm^{-1}.

2.3.2. Carboxyl contents of CNF-MA

The carboxyl contents of untreated CNF and CNF grafted with maleic acid were measured by means of conductometric titration. The CNF suspension with an oven-dry weight of 1 g was diluted with deionized water. 2 mL HCl (0.1 M) and 5 mL of NaCl (10 mM) were added and the total volume was adjusted to 500 mL. After sufficient mixing to obtain a stable suspension, the mixture was titrated with 0.1 M NaOH. The typical titration curves are shown in Fig. 2-7. The amounts of carboxyl groups were calculated using Eq. (2-1).

$$C = \frac{(V_1 - V_0) \times C_{NaOH}}{m} \quad \text{Eq. (2-1)}$$

In this equation, C is the carboxyl content (μmol/g), V_1 and V_0 are the equivalent volumes of the added NaOH solution (mL), C_{NaOH} is the concentration of the NaOH solution (mol/g), and m is the dry weight of the CNF (g).

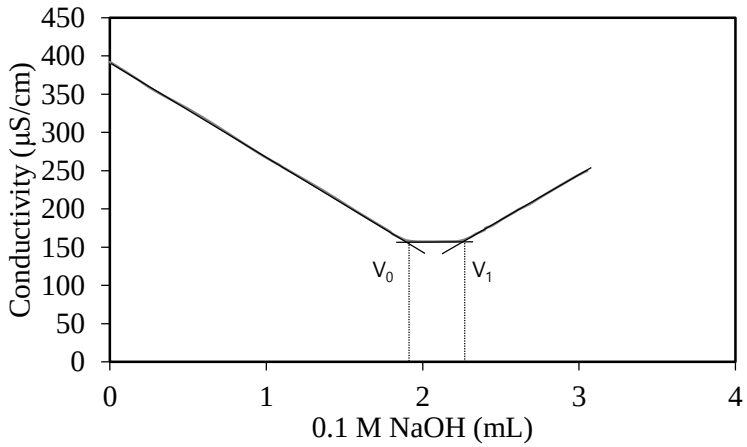

Fig. 2-7. Typical conductometric titration curve.

2.3.3. Moisture sorption measurement

Saturated salt solutions were used to adjust the relative humidity of air. In this research, three types of saturated salt solutions were placed in a humidity chamber (Table 2-1). Inside the humidity chamber, a weighing scale was also placed. The aerogels after drying at 120 ℃ for 24 hours were transferred into the humidity chamber and changes in the weights were recorded using a video camera. The moisture content of the CNF aerogel was calculated from Eq. (2-2) for each period of time.

$$\text{Moisture content}, \% = \frac{W - W_0}{W} \times 100 \quad \text{(2-2)}$$

Here, W is the weight of the CNF aerogel and W_0 is the dry mass of the CNF aerogel (g).

Table 2-2. Saturated salt solution and relative humidity

Saturated salt solution	Relative humidity of air (% RH at 23℃)
LiCl	15
$CaCl_2$	37
NaCl	75

2.3.4. Compressive strength and shape recovery test

To evaluate the compressive strength and shape-recovery performance of the cross-linked CNF aerogel, a texture analyzer (TA XT Plus, Stable Micro Systems, Ltd.) was used. A CNF aerogel cube was placed between the glass bottom plate and a cylindrical probe with a diameter of 50 mm. The compressive force was measured with a 50 kg load cell.

Fig. 2-8. Picture of texture analyzer (left) and cylindrical probe (right)

The compressive strength of a material is defined as the largest compressive force that the material can tolerate without fracturing. However, as CNF aerogel is a sponge-like material that can be compressed to more than 90 % of its original dimensions; thus, no fracture point or inflection point on the strain curve was observed, as shown in Fig. 2-9. Therefore, in this research, the compressive strength of the CNF aerogel was evaluated as the stress required to compress the aerogel to a strain level of 90 %. In the compressive strength test, the probe speed was adjusted to 1 mm/sec.

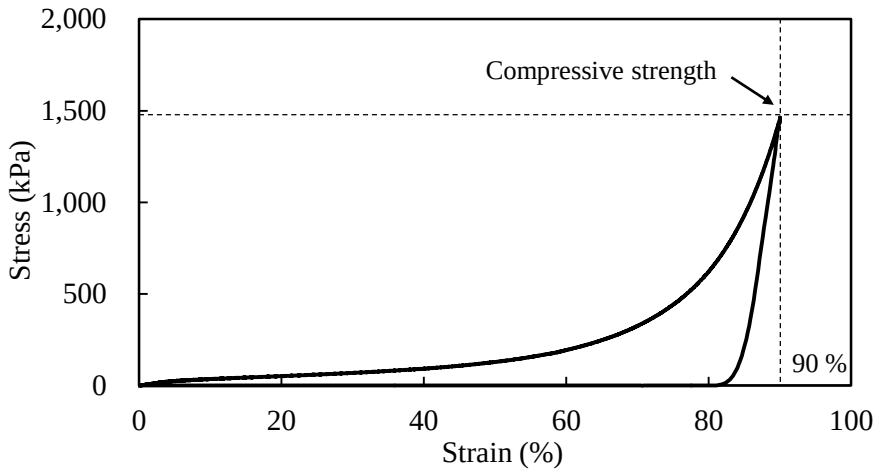

Fig. 2-9. Stress-strain curve of cross-linked CNF aerogel

For a quantitative evaluation of the shape-recovery performance of the cross-linked CNF aerogel in a wet state, a texture profile analysis (TPA) was carried out. This test consists of two cycles of compression of a sample. Springiness is described as the rate at which a deformed material recovers to its original condition after the removal of the deforming force. This is determined by Eq. (2-3). That is, when the springiness value is closer to one, the CNF aerogel easily recovers to its original shape after compression.

$$\text{Springiness} = \frac{T_2}{T_1} \qquad (2\text{-}3)$$

Here, T_1 is the compression time of the first compression cycle and T_2 is that of the second compression cycle.

For the TPA test, the probe speed was adjusted to 0.5 mm/sec. The interval time between the first compression step and the second compression step was 5 seconds.

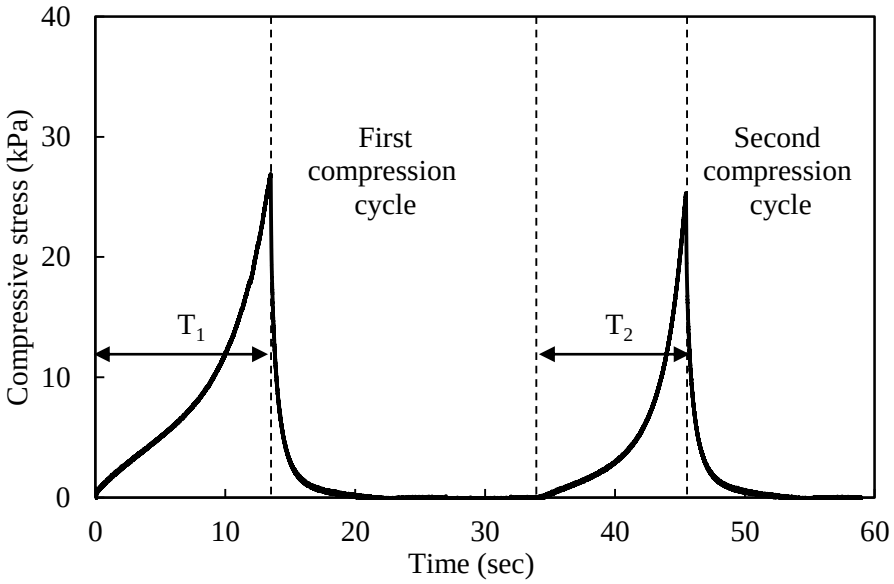

Fig. 2-10. TPA curve of cross-linked CNF aerogel in wet state

2.3.5. Cross-sectional observation of the CNF aerogel

Cross-section images of the CNF aerogel were obtained using a scanning electron microscope (SEM, Auriga, Carl Zeiss AG). The aerogel samples were frozen at -196 ℃ using liquid nitrogen and were then fractured. The samples were attached onto sample stubs with double-sided adhesive conductive carbon tape with the fracture surface upward, and a platinum layer 5 nm thick was deposited using a sputter coater.

2.3.6. Specific surface area

The specific surface areas of the aerogels were determined using nitrogen adsorption/desorption measurements (ASAP 2020, Micromeritics Instruments Co.) at a temperature of -196 ℃. The samples were dried at 105 ℃ for 24 hours to remove any moisture. Before the adsorption process, the specimens were degased at 120 ℃ for 4 hours for the complete elimination of moisture. Both adsorption and desorption isotherms were measured, and the surface area was determined from the adsorption curve by the Brunauer-Emmett-Teller (BET) method.

3. Results and Discussion

3.1. Esterification of CNF with maleic acid

The cross-linking of cellulose using maleic acid and hypophosphite ions takes place in two separate reactions. The first step of the cross-linking of CNF is an esterification reaction between maleic acid and the hydroxyl group of cellulose. This reaction scheme is shown in Fig. 2-12. First, maleic acid in an aqueous solution forms a five-membered cyclic anhydride by the dehydration of two carboxylic groups. This intermediate reacts with the hydroxyl group of cellulose, forming the ester linkage.

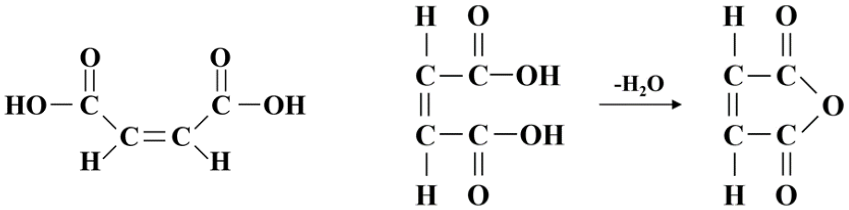

Fig. 2-11. Maleic acid (left) and formation of five-membered cyclic anhydride by dehydration of two carboxylic groups of maleic acid.

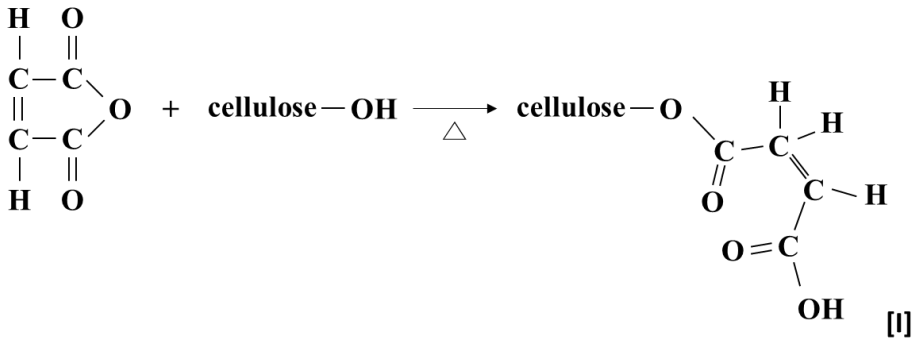

Fig. 2-12. Esterification between maleic acid and hydroxyl group of cellulose

During this esterification reaction, sodium hypophosphite is used as a catalyst. According to research by Yang et al. (2010), the degree of esterification between maleic acid and cotton fiber can be evaluated by the intensity of the ester carbonyl bond peak around 1730 cm^{-1} in the FT-IR spectrum. When cotton fabric was treated with only maleic acid at 130 ℃, the ester carbonyl band intensity was 0.11. The reaction degree was increased by the addition of sodium hypophosphite, and the maximum band intensity was 0.49. In this research, sodium hypophosphite corresponding to 5 wt % of maleic acid was added to the reaction mixture as a catalyst.

The FT-IR spectra of the maleic-acid-treated CNF (CNF-MA) are shown in Fig. 2-13. As the amount of maleic acid was increased, the peak intensity at 1570 cm^{-1} was increased. Due to the NaOH treatment, the carboxylic groups of CNF and the grafted maleic acid were converted to carboxylate anion; this peak is assigned to the C=O stretching vibration of the ester linkage. As a result, the FT-IR spectra indicate that maleic acid was grafted onto CNF through an esterification process.

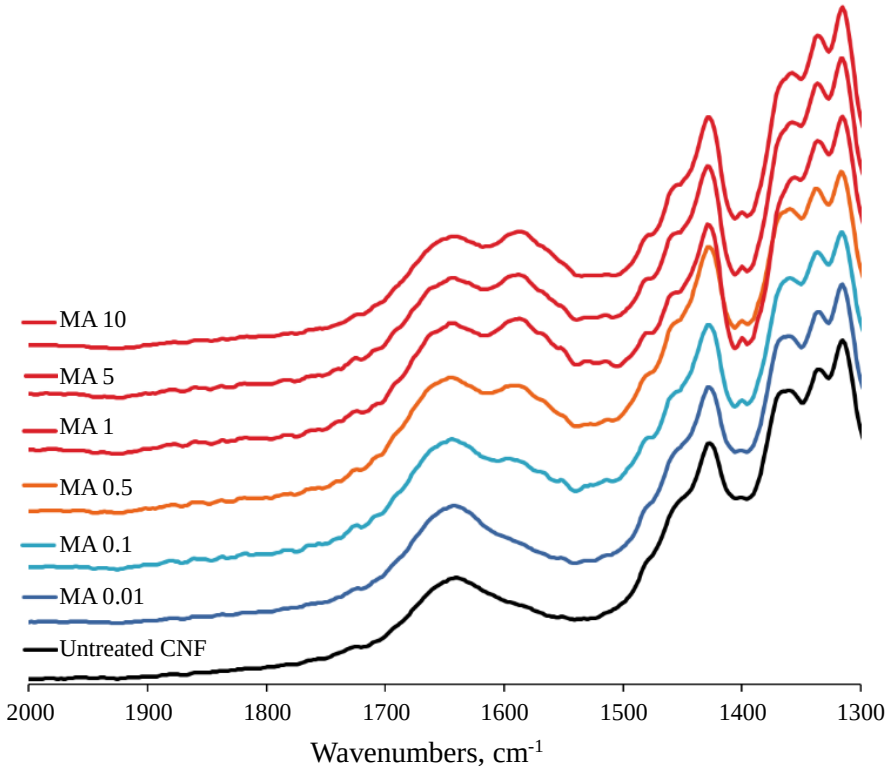

Fig. 2-13. FT-IR spectra of maleic acid treated filter paper CNF

However, in this FT-IR experiment, Whatman No. 2 filter paper was used as a starting material for the CNF to prepare pure cellulose raw material. When CNF made of hardwood kraft pulp was used, the FT-IR spectrum of CNF-MA exhibited a very small difference compared to that of the untreated CNF, as shown in Fig. 2-14. This slight difference with regard to the FT-IR spectrum of the CNF-MA appeared to be due to the chemical composition of the CNF. In this work, bleached hardwood kraft pulp was used as a raw material to prepare the CNF. It contains mostly hemicellulose and lignin, at 20 %. It appeared that the carboxylate peak of CNF-MA at 1570 cm^{-1} was overlapped by the inherent peak from the hemicellulose and lignin.

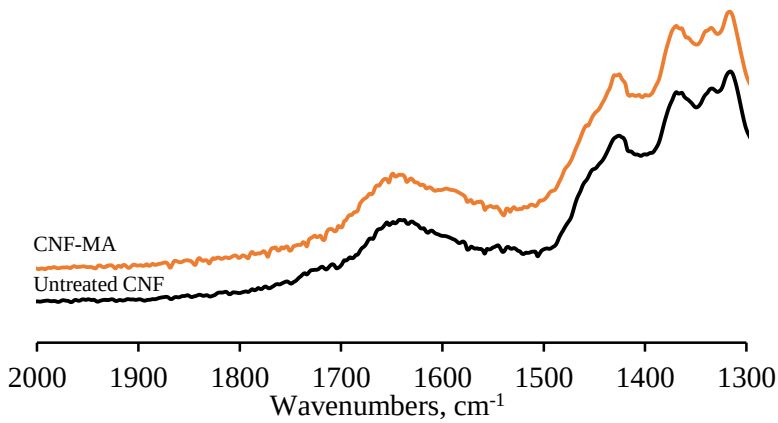

Fig. 2-14. FT-IR spectra of untreated CNF and CNF-MA

In order to form an ester linkage with polycarboxylic acid and the hydroxyl group of cellulose, the formation of five-membered cyclic anhydride as a reactive intermediate is required. Because maleic acid is bicarboxylic acid, however, it is not able to react with other hydroxyl groups of cellulose once grafted onto the cellulose with an ester linkage. Therefore, the amount of grafted maleic acid was determined by measuring the carboxyl group content by means of the conductometric titration of the CNF suspension. Table 2-3 shows the carboxyl group content of the maleic-acid-grafted CNF.

Table 2-3. Carboxyl group content of maleic acid grafted CNF

Maleic acid	Molar ratio of MA to AGU	Carboxyl group content μmol/g
Untreated CNF		44
CNF-MA	0.1	66
	0.5	79
	1	94
	5	112
	10	117

3.2. Cross-linking of cellulose

Because polycarboxylic acids such as 1,2,3,4,-butanetetracarboxylic acid (BTCA) form multiple ester linkages with cellulose, they have widely been used as a cross-linking agent in durable press finishing to produce wrinkle-resistant cotton fabric since the 2000s (Yang et al. 2010, Cho et al. 2003). In contrast, maleic acid is a bifunctional carboxylic acid, and once it forms an ester linkage with cellulose, it cannot form a cyclic anhydride intermediate; therefore, it also cannot produce a cross-linkage of cellulose. However, the C=C double bond of maleic acid when grafted onto cellulose can be reacted with hypophosphite to form a covalent bond above 140 ℃; thus, the cross-linkage of cellulose is produced, as shown in Fig. 2-15.

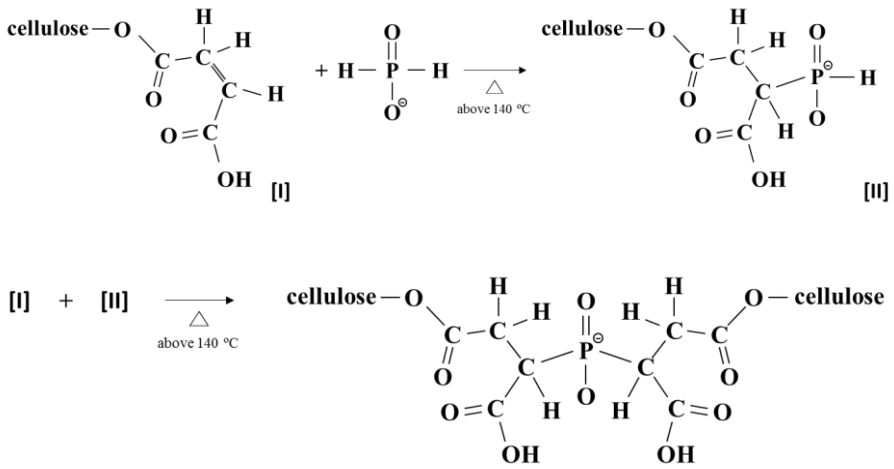

Fig. 2-15. Cross-linking of cellulose by the reaction between maleic acid and hypophosphite

3.3. Internal structure of the CNF aerogel

Water in the CNF suspension is replaced with air without a collapse or shrinkage of the network structure through rapid freezing and freeze-drying; thus, CNF aerogel is produced (Aulin et al. 2010). Therefore, the apparent volume of the resultant CNF aerogel is considered to be the original volume of the CNF suspension in the mold. The density is proportional to the initial solids content of the CNF suspension. The densities of the CNF aerogels are presented in Table 2-4. The specific surface area of the CNF aerogel was 19.5 m^2/g when the density of the cross-linked CNF aerogel was 21.7 kg/cm^3. The specific surface areas were low compared to other organic/inorganic aerogels produced by the sol-gel process with a subsequent supercritical CO_2 drying process (400 – 654 m^2/g, Cai et al. 2012), but these values were in good agreement with previously reported values from freeze-dried CNF aerogels (15 – 45 m^2/g at a density of 7 – 103 kg/m^3, Sehaqui et al. 2010)

Table 2-4. Density of CNF aerogel and specific surface area

Solids content of CNF hydrogel (wt %)	1.0	1.5	2.0	2.5	3.0
Density of CNF aerogel (kg/m^3)	11.2	16.2	19.9	26.7	31.5

Cross-sectional images of the cross-linked CNF aerogel with a density of 21.7 kg/m^3 are presented in Fig. 2-16. The internal network structure of the cross-linked CNF aerogel was composed of nanopapers. As shown in Fig. 2-17, these nanopapers were composed of randomly oriented cellulose nanofibers. This type of nanopaper structure is commonly found in cellulose aerogels prepared by the freeze-drying of a CNF suspension (Syverud et al. 2011, Sehaqui et al. 2010, 2011, Cervin et al. 2012, Aulin et al. 2010). During the freeze-drying of the CNF suspension, randomly distributed nanofibers are pushed out by growing ice crystals and develop film-like cellulose nanopapers (Svagan et al. 2008, Chen et al. 2011).

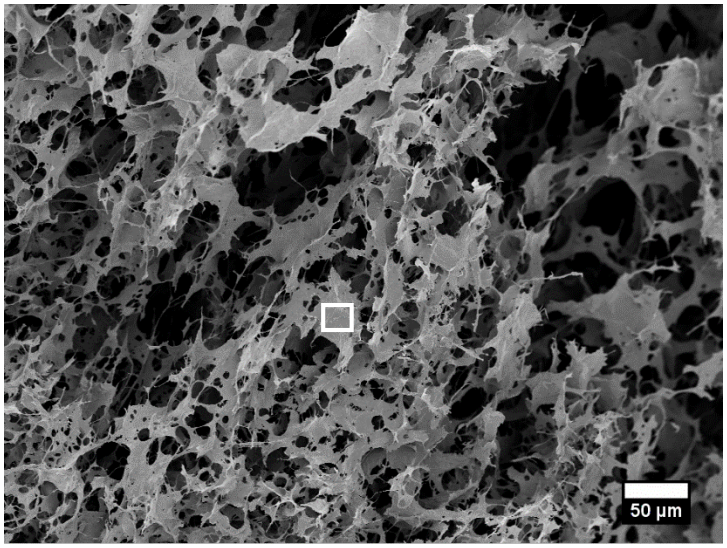

Fig. 2-16. SEM image of internal networks structure of the cross-linked CNF aerogel.

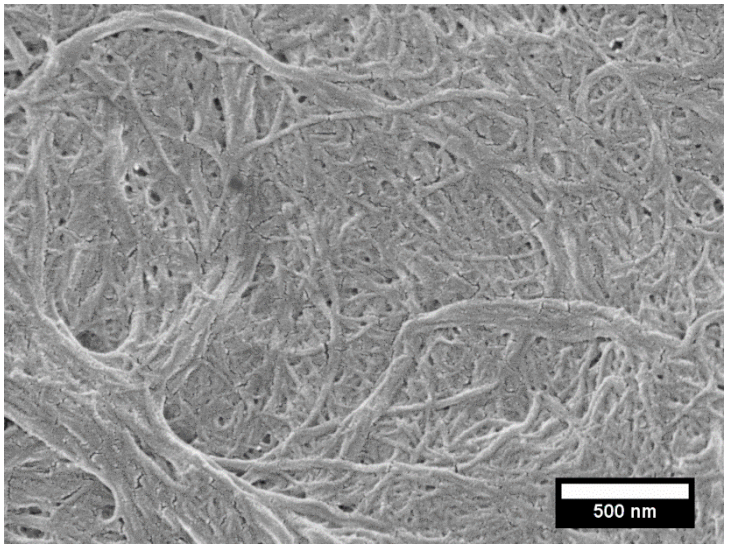

Fig. 2-17. High magnification SEM images of a lamella of cross-linked CNF aerogel indicated with white box in Fig. 2-16.

3.4. Response of the cross-linked CNF aerogel to moisture

As the pulp fiber is disintegrated into cellulose nanofibril, the specific surface area of the fiber is drastically enlarged, and the number of hydroxyl and carboxyl groups exposed to the fiber surface also increases. Compared to typical handsheet paper with a basis weight of 150 g/m^2, the cross-linked CNF aerogel exhibits a much higher equilibrium moisture content, as shown in Fig. 2-18.

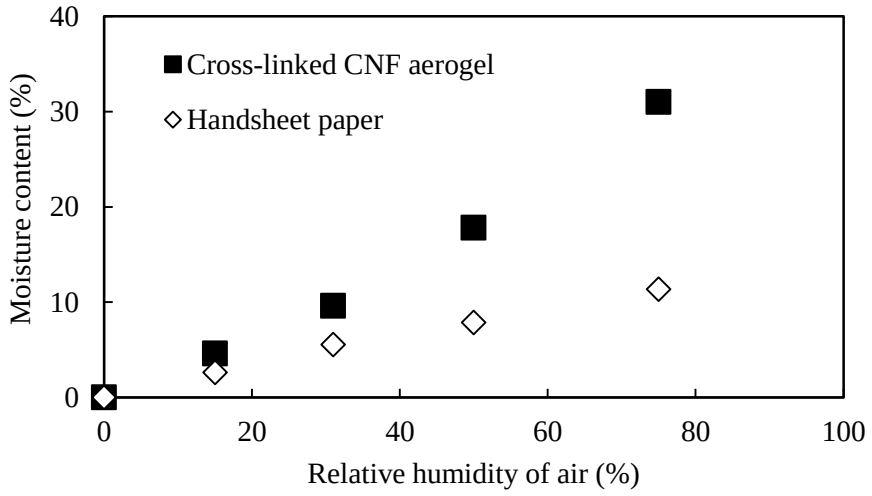

Fig. 2-18. Equilibrium moisture content of cross-linked CNF aerogel and handsheet paper according to relative humidity of air

The nanofibrillar network structure of a typical CNF aerogel is built by hydrogen bonds and physical entanglements between adjacent CNFs. Accordingly, when a typical CNF aerogel is exposed to moisture, the interfibrillar hydrogen bonds are easily broken and the entire network structure of the aerogel is weakened considerably. As shown in Fig. 2-19, untreated and cross-linked CNF aerogels were immerged in deionized water. After mild mixing for a 1 minute with a magnetic stirrer, the untreated CNF aerogel disintegrated and individual nanofibrils were dispersed in water. On the other hand, the cross-linked CNF aerogel maintained its original structure. This indicates that the covalent cross-linking of cellulose was successfully formed through the treatment with maleic acid and hypophosphite.

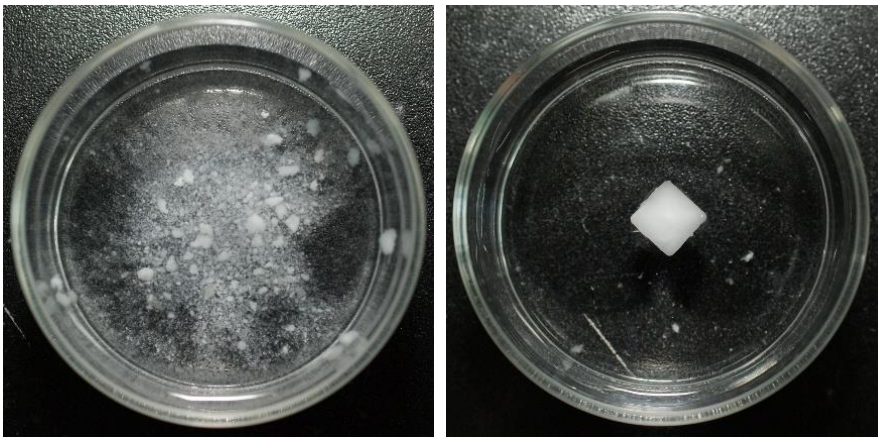

Fig. 2-19. Pictures of untreated CNF aerogel (left) and cross-linked CNF aerogel (right) after 1 min magnetic stirring in water.

As a result of the improved aerogel network stability in water, the cross-linked CNF aerogel exhibited good water absorption capability. A water absorption test was carried out by immersing the cross-linked CNF aerogel into deionized water. The cross-linked CNF aerogel is composed of hydrophilic cellulose and numerous internal pores. When the cross-linked CNF aerogel was immersed in water, it instantly absorbed water by the wetting of individual fibers and by capillary action. However, shrinkage of the cross-linked CNF aerogel was observed during the initial stage of absorption. As more water penetrated into the interior of the cross-linked CNF aerogel, it recovered its original shape. At the initial stage of absorption, the internal pores of the cross-linked CNF aerogel were partially filled with water, and an air-water interface existed. As a result, the surface tension of water was applied to the cross-linked CNF network and the aerogel was compressed. The cross-linked CNF network was not destroyed, and endured this compression through covalent cross-linking. As more water was absorbed and the internal pores were filled by water, the volume of water was increased and the air-water interface disappeared due to the expansion of the aerogel. In contrast to the cross-linked CNF aerogel, the untreated CNF aerogel was built with hydrogen bonds only; consequently, the network structure was irreversibly destroyed and collapsed due to the absorbed water.

In Fig. 2-20, the water-absorbing capabilities of the cross-linked CNF aerogel with the density are presented. The volume of absorbed water corresponded to the internal volume of the aerogel; therefore, the water-absorbing capability in terms of the volume-to-volume ratio was maintained at a value close to one. In contrast, the water-absorbing capability in terms of the

weight-to-weight ratio increased as the density of the cross-linked CNF aerogel decreased. For the sample with the lowest density of 11.3 kg/m^3, the compression of the cross-linked CNF aerogel during absorption was not fully recovered because the network strength of the cross-linked CNF aerogel was not strong enough to resist the compressive force driven by the surface tension of the absorbed water. This partial collapse of the CNF aerogel during the absorption process resulted in a decrease of the internal pore volume and water-absorbing capacity.

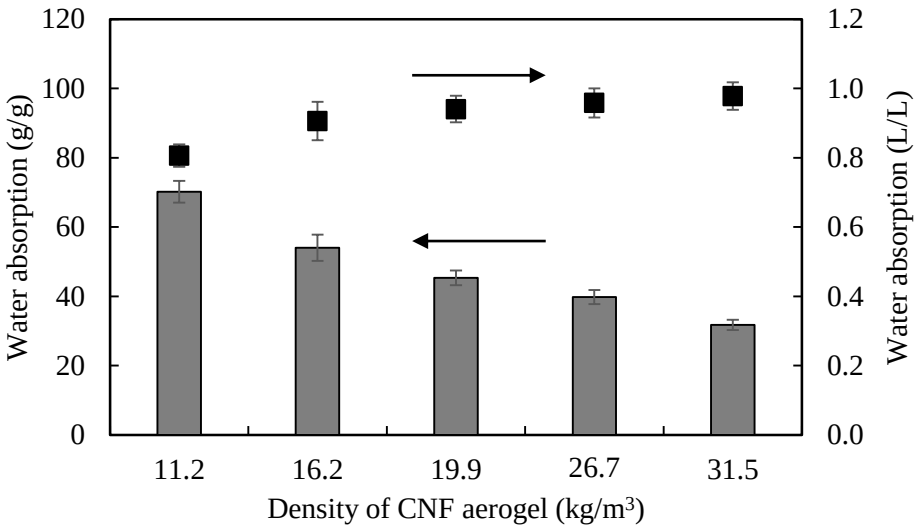

Fig. 2-20. Water absorbing capability of cross-linked CNF aerogel

3.5. Mechanical strength and shape recovery of the cross-linked CNF aerogel

In Fig. 2-21, the stress-strain curves of the untreated and cross-linked CNF aerogel with a density of 25.7 kg/m^3 and a moisture content of 17.8 % are compared. As shown in Table 2-5, the cross-linked CNF aerogel shows an increase in the compressive strength of approximately 30 % compared to the untreated CNF aerogel in a dry state. This change in the compressive strength indicates that covalent cross-linking of the CNF formed due to the reaction between the maleic acid and the hypophosphite.

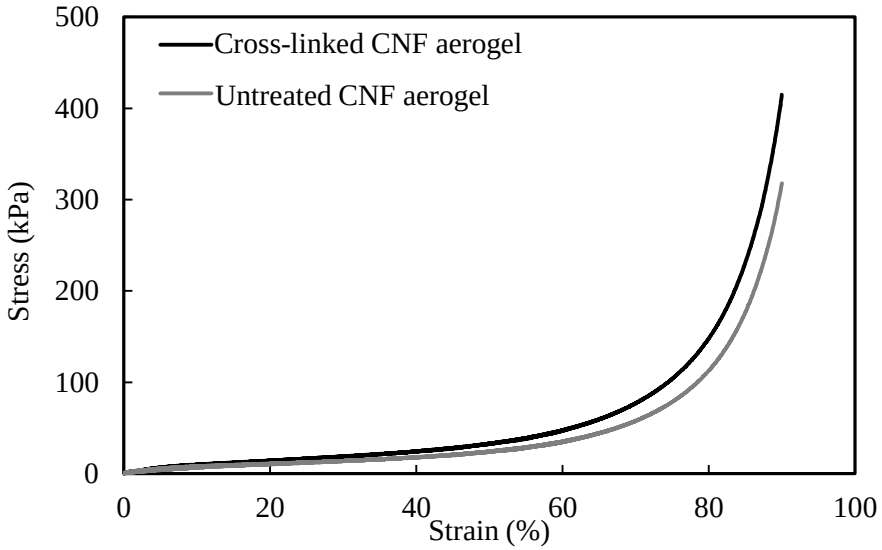

Fig. 2-21. Stress-strain curves of untreated and cross-linked CNF aerogel in dry state.

Table 2-5. Compressive strength of untreated and cross-linked CNF aerogel in dry state.

Specimen	Compressive strength in dry state (kPa)
Untreated CNF aerogel	317
Cross-linked CNF aerogel	417

A fiber network of paper and paperboard was built by the hydrogen bonds between adjacent fibers. As the relative humidity increases, the cellulosic material adsorbs more moisture. Adsorbed water molecules on the surface of the fiber hinder the formation of interfibrillar hydrogen bonds, thus decreasing the mechanical strength (Kang and Kim 2012, Kim et al. 2006, Song et al. 2005, Lee et al. 2002). The compressive strength of the cross-linked CNF aerogel was exponentially decreased as the moisture content increased, as shown in Fig. 2-22 and 23. This drastic decrease in the compressive strength indicates that a considerable portion of the CNF network structure still consists of hydrogen bonds after the cross-linking treatment. Nevertheless, the compressive strength of the cross-linked CNF aerogel in a fully wet state was increased by about 50 % compared to that of the untreated CNF aerogel, as shown Fig. 2-24 and in Table 2-6.

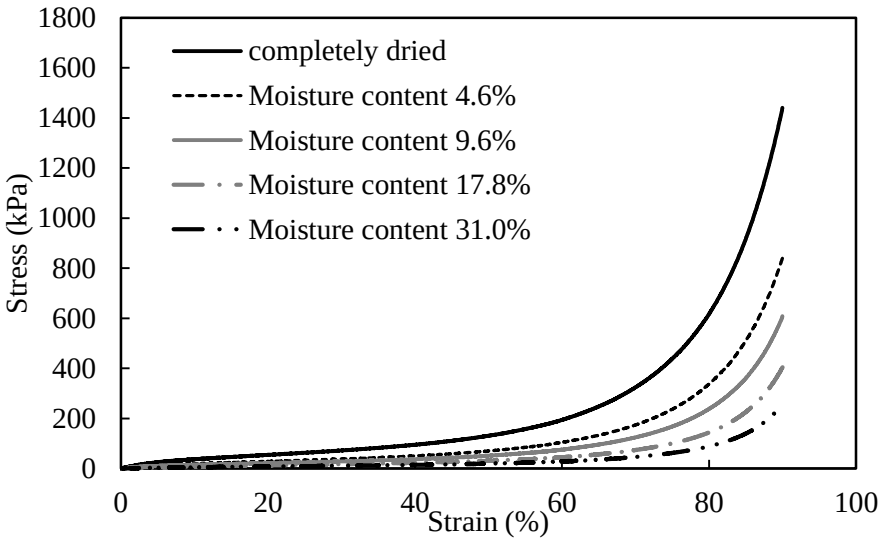

Fig. 2-22. Stress-strain curves of cross-linked CNF aerogel according to the moisture content.

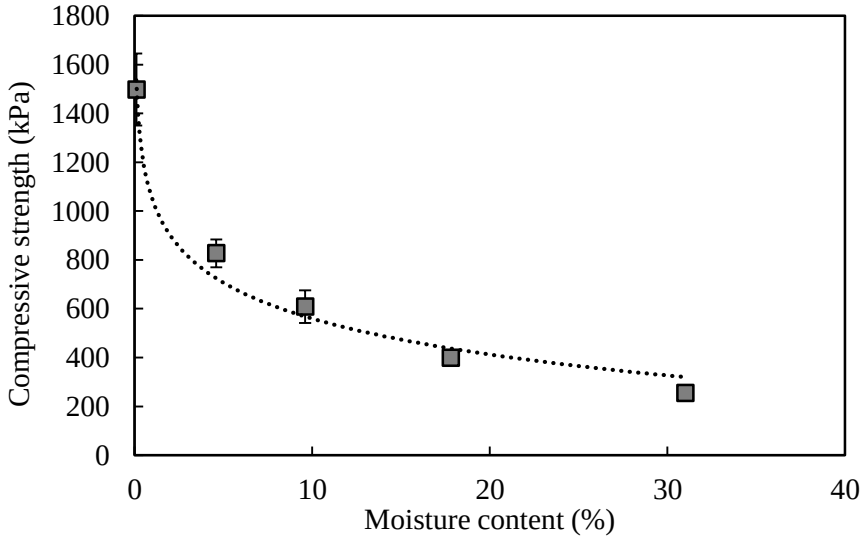

Fig. 2-23. Compressive strength of cross-linked CNF aerogel according to moisture content.

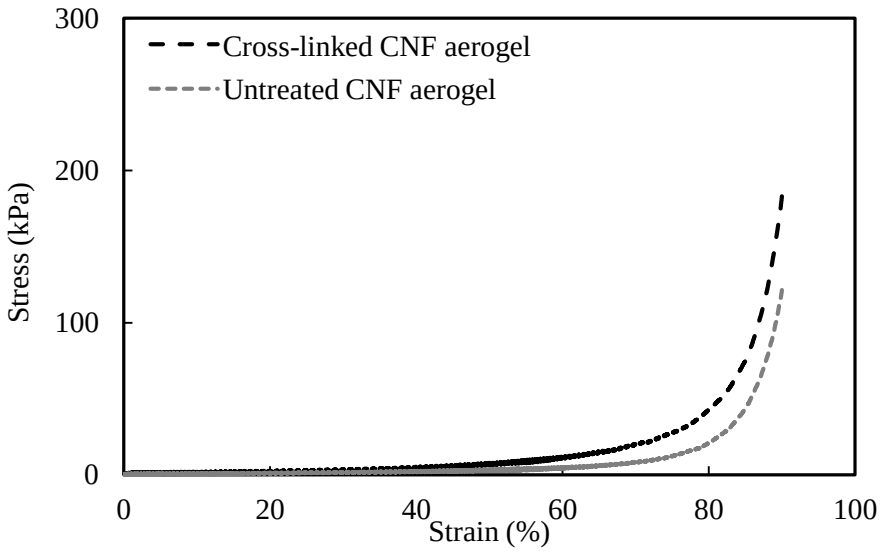

Fig. 2-24. Stress-strain curves of untreated and cross-linked CNF aerogel in wet state

Table 2-6. Compressive strength of untreated and cross-linked CNF aerogel in wet state.

Specimen	Compressive strength in wet state(kPa)
Untreated CNF aerogel	120
Cross-linked CNF aerogel	180

In addition to the increased compressive strength, the cross-linked CNF exhibits remarkable shape-recovery behavior after compressive deformation. In a dry state, the cross-linked CNF aerogel showed plastic deformation and remained in a compressed shape, as shown in Fig. 2-25. By dropping a water droplet onto the compressed dry cross-linked CNF aerogel, it recovered nearly 70 % of its original shape within a few seconds. This shape-recovery characteristic of the cross-linked CNF aerogel in a wet state was evaluated by a TPA test. As shown in Fig. 2-26, the wet cross-linked CNF aerogel recovered its shape after compression, while the untreated CNF aerogel remained in a compressed shape. The shape-recovery behavior of the cross-linked CNF aerogel in a wet state is expressed in the time-stress curve generated from the TPA test in Fig. 2-27. Quantitatively, the springiness value of the cross-linked CNF aerogel was 0.78, while that of the untreated CNF aerogel was only 0.33.

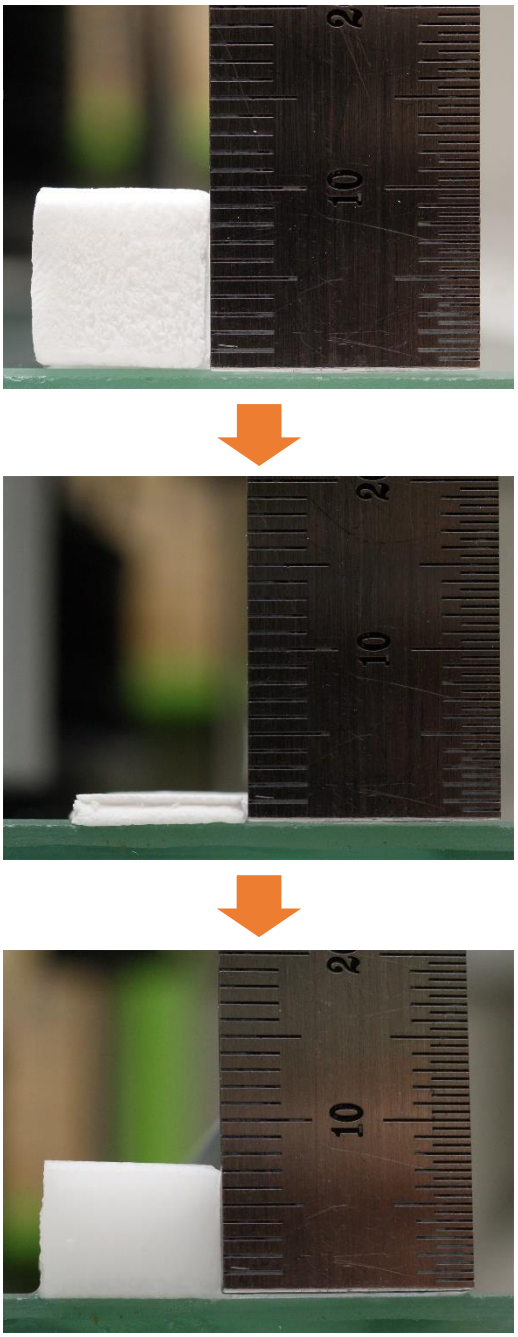

Fig. 2-25. Shape recovery of cross-linked CNF aerogel by water absorption.

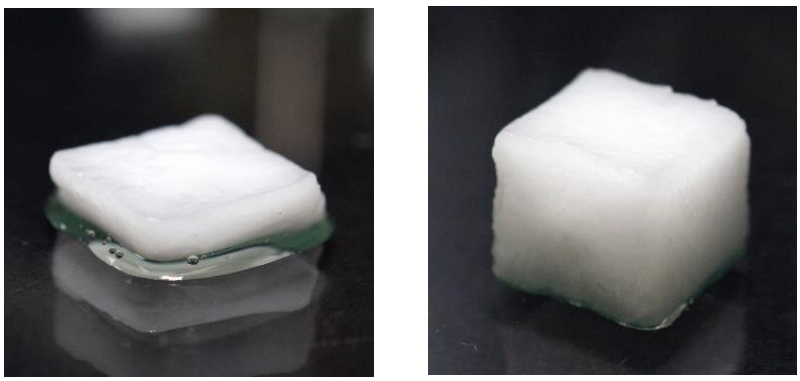

Fig. 2-26. Untreated (left) and cross-linked (right) CNF aerogel after compression in wet state

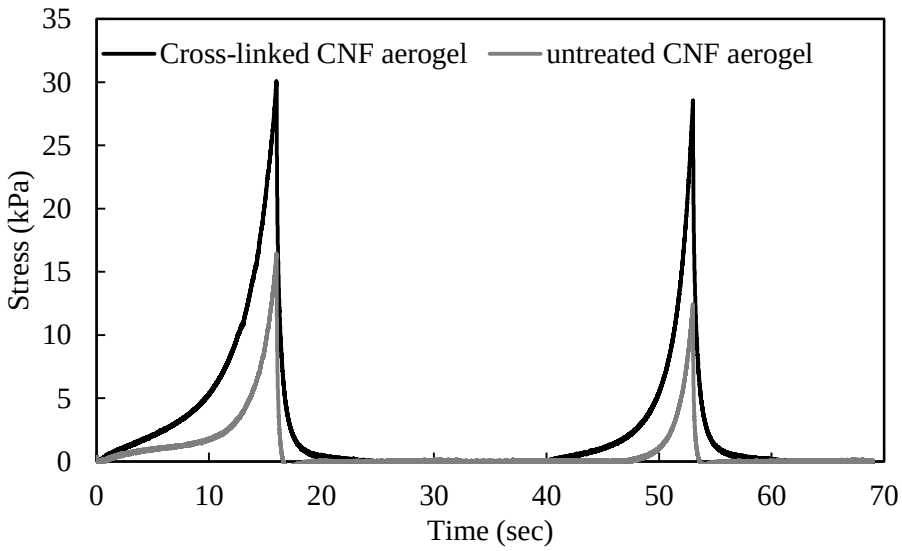

Fig. 2-27. TPA curves of untreated and cross-linked CNF aerogel in wet state

Zhang et al. (2012) explained the shape-recovery characteristics of cross-linked CNF aerogels in terms of the interaction between the absorbed water and the CNF. The compression of the fiber network of CNF aerogels arises from the bending of individual fibers, interfibrillar bonding, and from friction between adjacent fibers and the physical entanglement of fibers.

Compressive deformation of the fiber itself in the longitudinal direction can be neglected, and only the bending of the fiber is taken into account due to its high aspect ratio. However, the elastic modulus of the crystal region of cellulose is known to be between 130 GPa and 250 GPa (Zimmermann et al. 2004, Sakurada et al. 1962), while that of the amorphous region is quite low, reportedly at 12.2 GPa (Wang et al. 2014) or 10.4 GPa (Chen et al. 2004) according to molecular modeling research. As a result, the bending of the CNFs is confined to the amorphous region. When the cross-linked CNF aerogel is exposed to water, individual CNFs become wet and the amorphous region of cellulose swells somewhat. The swollen amorphous region forces an extension, and the original shape of the CNF is recovered after the external force is removed.

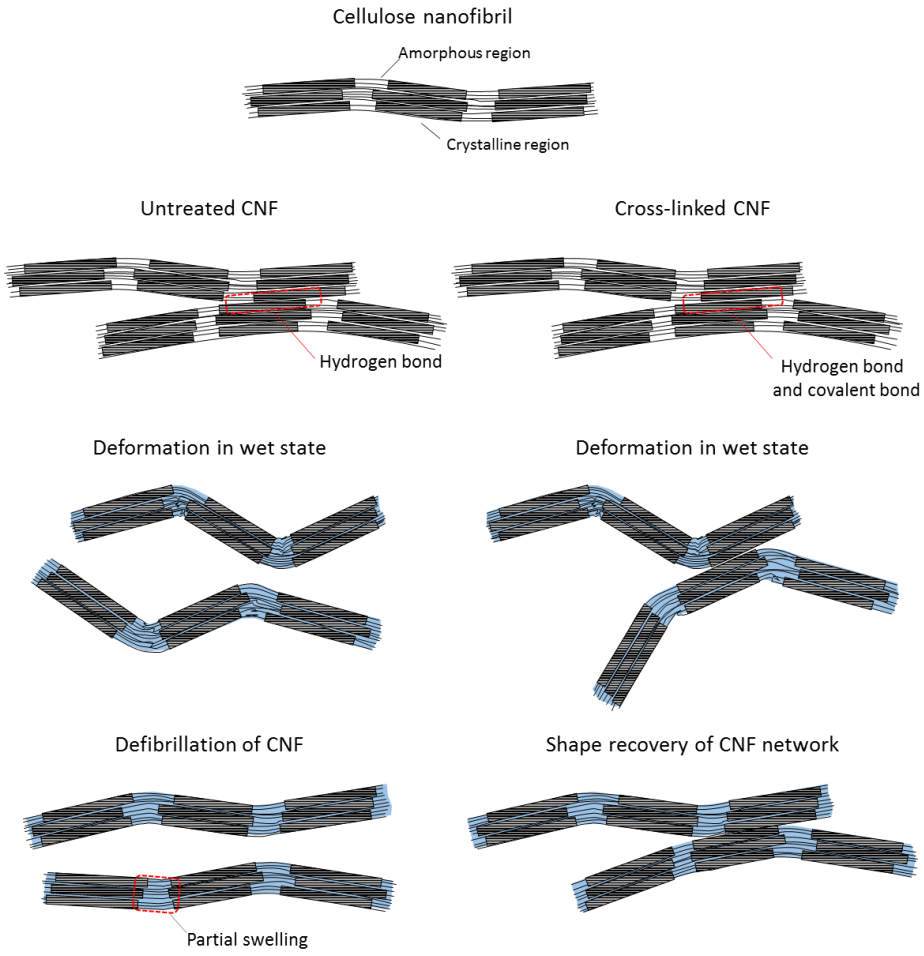

Fig. 2-28. Shape recovery of cross-linked CNF in wet state

The three-dimensional structure of the CNF aerogel is composed of two-dimensional nanopapers, and this fiber network consists of hydrogen bonds between adjacent cellulose nanofibers. In a wet state, the hydrogen bonds are greatly reduced. When a typical CNF aerogel is exposed to external force in a wet state, the number of interfiber bonds is greatly reduced and the structure cannot withstand the shear forces induced by the compression of the fiber network and the shape recovery of individual cellulose nanofibers. This results in the destruction of the entire network structure. Specifically, the breakage of the CNF network is concentrated at the connection points in the nanopapers due to the lower mechanical stability of these regions compared to that of CNF nanopaper itself.

In contrast, part of the fiber network of the cross-linked CNF aerogel consists of the covalent cross-linkage of cellulose, and the network structure possesses improved mechanical stability in a wet state. As a result, the cross-linked CNF aerogel is able to maintain its original interfiber network structure when it is compressed. When the external force is removed, the deformed individual fibers recover their original shape, and this expanding force is applied to the entire network. As the compressed CNF nanopapers recover their internal pore structure, additional water penetrates into the pores. As a result, additional hydrodynamic force is generated, leading to further recovery.

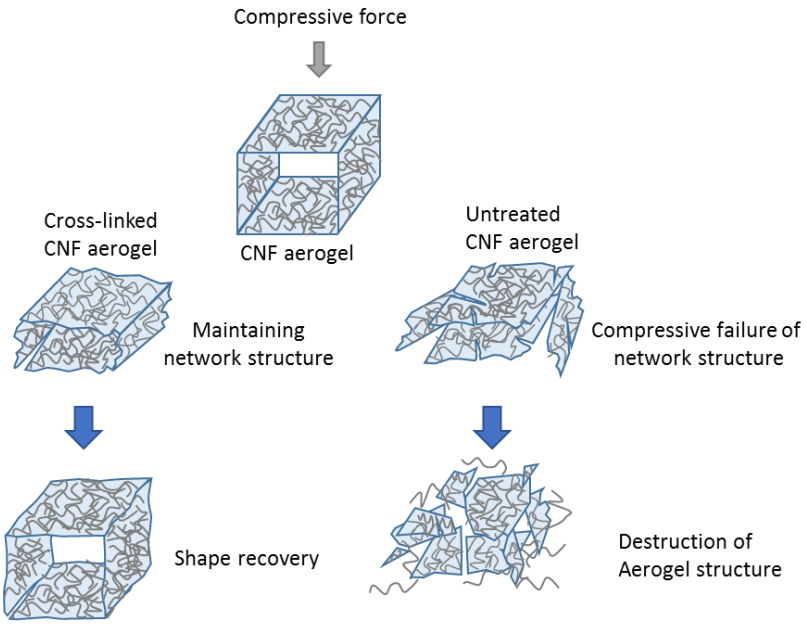

Fig. 2-29. Shape recovery of cross-linked CNF aerogel and redispersion of untreated CNF aerogel after compression in wet state.

3.6. Effect of the reaction condition on the cross-linked CNF aerogel properties

The dosages of maleic acid and sodium hypophosphite and the curing temperature and time were varied during the preparation of the cross-linked CNF aerogel. To investigate the effect of these reaction conditions on the properties of the cross-linked CNF aerogel, the springiness value from the TPA test was used as an indicator of the degree of cross-linking.

As part of the preparation of the cross-linked CNF, the dosage of maleic acid was adjusted during the esterification of the CNF. The molar ratio of maleic acid to AGU for the CNF was varied from 0.1 to 10. For each maleic acid dosing level, other reaction conditions were identical; the dosage of sodium hypophosphite was 5 wt % of that of maleic acid, the added amount of sodium hypophosphite was 20 wt % of that of CNF-MA after the centrifugal washing step, the temperature and time were respectively 170 ℃ and 10 minutes during each curing step. The solids content of the CNF-MA suspension with sodium hypophosphite added to it was 2.5 wt %. As shown in Fig. 2-30, when the ratio of maleic acid to AGU was 5, the springiness value of the cross-linked CNF aerogel reached its maximum value, but the difference was not significant.

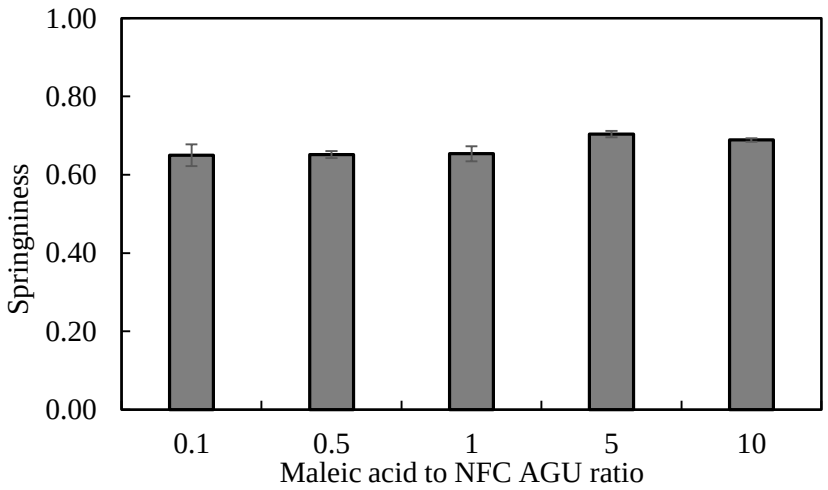

Fig. 2-30. Springiness values of cross-linked CNF aerogel with dosage of maleic acid

After the esterification of CNF with maleic acid, untreated chemicals were removed by centrifugal washing and sodium hypophosphite was then added. At this stage, the dosage of sodium hypophosphite was adjusted from 10 to 40 wt % of that of CNF-MA. The molar ratio of maleic acid to AGU for the CNF was 10 in the esterification stage, and the curing temperature and time were respectively 170 ℃ and 10 minutes during the curing step. The solids content of the CNF-MA suspension with sodium hypophosphite added to it was adjusted to 2.5 wt %. In this sample group, the springiness value of the cross-linked CNF aerogel was highest when the dosage of sodium hypophosphite was 20 wt % of that of CNF-MA, as shown in Fig. 2-31. Above 20 wt %, the springiness decreased as the dosage of sodium hypophosphite was increased. Thus, the interfiber bonding of adjacent fibrils was hindered by the excessive amount of sodium hypophosphite.

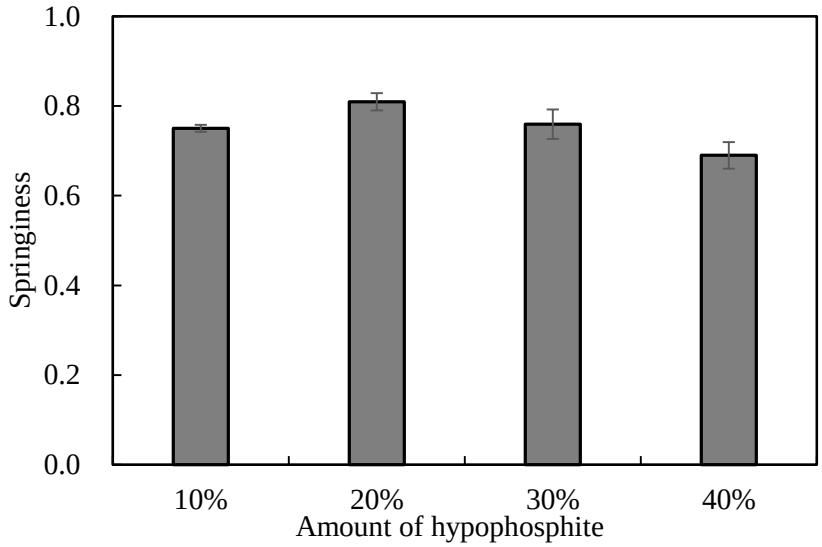

Fig. 2-31. Springiness value of cross-linked CNF aerogel with amount of sodium hypophosphite

To evaluate the effect of the curing condition, the temperature was adjusted from 120 to 170 ℃. In this case, the curing time was 10 minutes. As presented in Fig. 2-32, the springiness value increased continually as the curing temperature was increased. In addition, the curing time was varied from 1 to 30 minutes when the curing temperature was 170 ℃. As shown in Fig. 2-33, the springiness value reached its maximum point at 10 minute, maintaining the same level after a curing time of 30 minutes. To prepare the cross-linked CNF aerogel under this curing condition, the molar ratio of maleic acid to AGU for the CNF was 10 in the esterification stage, and the added amount of sodium hypophosphite was 20 wt % of that of CNF-MA after the centrifugal washing step. The solids content of the CNF-MA suspension with sodium hypophosphite added to it was adjusted to 2.5 wt %.

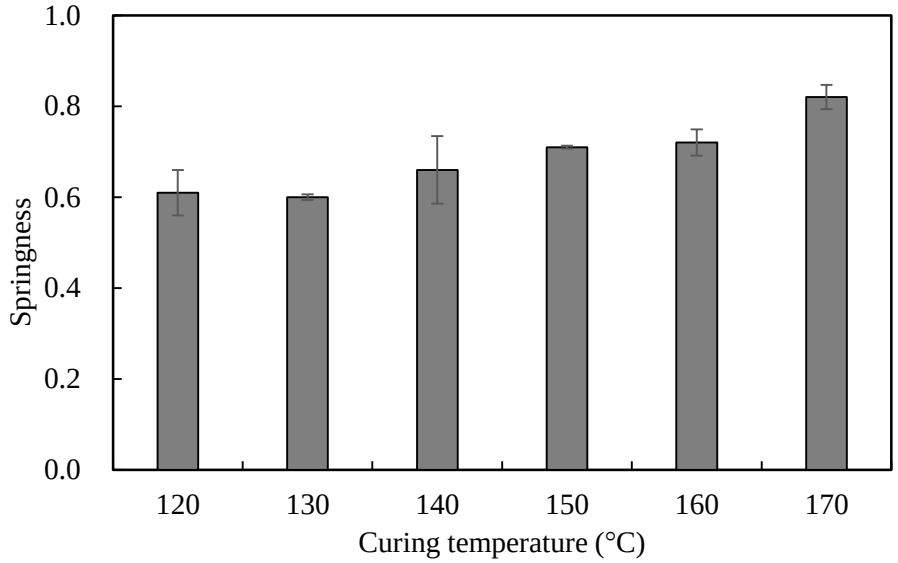

Fig. 2-32. Springiness value of cross-linked CNF aerogel with curing temperature

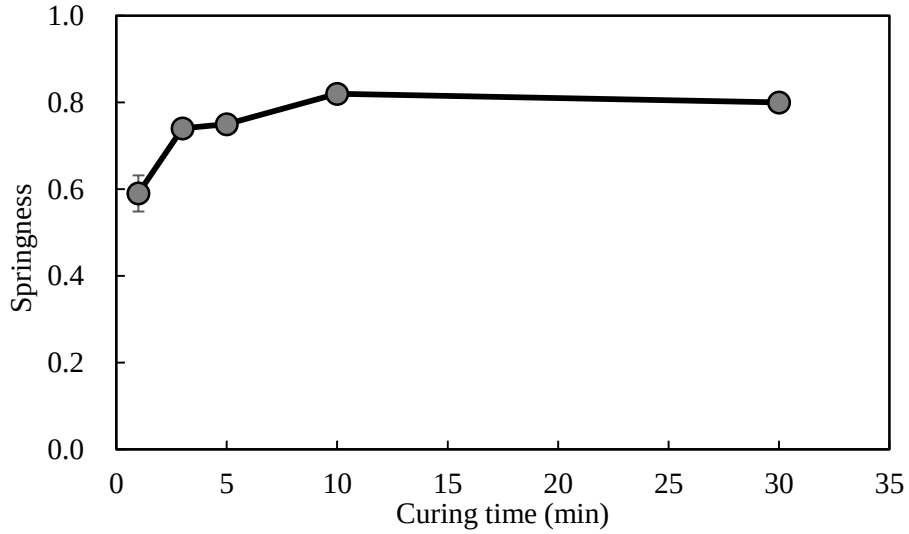

Fig. 2-33. Springiness value of cross-linked CNF aerogel with curing time

4. Summary

In this study, a cross-linked CNF aerogel was produced. As the cross-linking agents, maleic acid and hypophosphite were used. The cross-linking reaction consisted of two steps: 1) the esterification of CNF with maleic acid, and 2) the formation of a cellulose cross-linkage by a reaction between maleic acid and hypophosphite.

After the rapid freezing and freeze-drying of CNF suspension, ultralight and highly porous CNF-MA aerogels were produced. After a curing treatment of the produced CNF-MA aerogel, a cross-linked CNF aerogel was prepared. Its internal structure consisted of cellulose nanopaper with numerous open pores. The compressive strength of the cross-linked CNF was increased compared to an untreated CNF aerogel both a dry and a wet state. It also showed improved network stability toward moisture and water absorbency.

The cross-linked CNF aerogel showed plastic deformation behavior after compression in a dry state. However, it exhibited shape-recovery characteristics in a wet state. After compression in a wet state, the cross-linked CNF aerogel recovered its original shape within a few seconds, while the untreated CNF aerogel collapsed and did not recover its original shape. The shape-recovery performance was evaluated using the springiness value from a TPA test. The springiness value of the cross-linked CNF aerogel was 0.78, while that of the untreated aerogel was only 0.33. The shape-recovery characteristic of the cross-linked CNF aerogel was explained in terms of the interaction between the absorbed water and the CNF nanopaper.

Chapter 3

Cationic modification of cellulose nanofibrils

1. Introduction

Cellulose fibers have a negative charge due to the carboxyl group in their chemical composition. The anionic charge of cellulose fiber surface repels other anionic materials by electrostatic repulsive force.

However, the surface charge property of cellulose fiber can be modified by chemical means. The most common cationic treatment agents are epoxy-group moieties with a quaternary ammonium functional group. Upon a surface modification treatment using these chemicals, cationically modified cellulose will exhibit new functionalities. For example, Abbott et al. (2006) reported that cationic cellulose can be used as an anionic dye remover. Roy et al. (2007) reported antibacterial properties of cationic cellulose. These chemicals are also widely used for cationic starch processes (Nachtergaele et al. 1989).

In this study, the surface charge of CNF was modified to make it cationic. Glycidyltrimethylammonium chloride (GTMAC) was used as a cationic modification agent. The epoxy group of GTMAC reacted with the hydroxyl group of cellulose and formed an ether linkage. GTMAC-grafted CNF exhibited a positive charge due to the quaternary ammonium group of GTMAC. However, it is known that water in the reaction mixture significantly influences the reaction efficiency of the etherification reaction of epoxy-group moieties. Therefore, the CNF suspension was dewatered using pressurized dewatering equipment and the effects of the water content in the reaction mixture on the degree of substitution and the reaction efficiency were investigated.

2. Materials and methods

2.1. Preparation of CNF

Commercial bleached eucalyptus kraft pulp was used as a raw material. Dried pulp sheets were dispersed in deionized water and were refined using a laboratory valley beater as a mechanical pretreatment. After 10 minutes of disintegration, the pulp slurry was beaten for 12 minutes and 30 seconds to obtain a freeness value of 450 mL CSF. The beaten pulp slurry was concentrated until its solids content was 2 wt %. The beaten fiber suspension was processed using a grinder (Super Masscollider MKCA6-3, Masuko Sanguo Co.). The pulp fibers were then passed through a gap between a static ceramic grinding stone and a rotating grinding stone revolving at 1,500 rpm. The gap was adjusted to -60 μm, with 40 passes.

2.2. Dewatering of CNF suspension

In this process, the CNF suspension was dehydrated using pressurized dewatering equipment (Quro). A Whatman No. 2 filter paper was placed in the bottom of the cylinder as the filter media, after which approximately 100 g of the CNF suspension was transferred into the cylinder. Thereafter, the CNF suspension was pressed at 6 bar for 1 hour. As a result, a CNF pad was created with a solids content of about 7.5 wt%.

2.3. Preparation of cationic CNF

For the preparation of the cationic CNF, glycidyltrimethyl-ammonium chloride (GTMAC) was used as a cationization agent. As shown in Fig. 3-1, the GTMAC was composed of epoxy and quaternary ammonium groups. NaOH was used as a catalyst. These chemicals were obtained from Sigma-Aldrich and were used without further purification.

The dosage of GTMAC was calculated as the molar ratio of GTMAC and the anhydroglucose unit (AGU) of cellulose, under the assumption that the CNF was composed of only cellulose. The dosage of NaOH was 5 wt % of the dry mass of CNF.

The CNF pad was put in a plastic bag and mixed well with a 50 wt% NaOH solution by intensive hand kneading. This mixture was heated to 70 ℃ for 30 min using a hot water bath. The GTMAC was then added to the reaction mixture. This mixture was reacted at 70 ℃ for 4 hours in a hot water bath. During the reaction, the mixture was hand kneaded every 15 minutes. At the end of the reaction, the mixture was cooled down by adding deionized water. The unreacted chemicals and by-products were removed by centrifugal washing at 3000G for 10 min. The CNF pad was redispersed in deionized water and the subsequent centrifugal washing steps were carried out. This procedure was repeated 6 times. In this way, a GTMAC-treated-CNF (CNF-GTMAC) suspension was prepared.

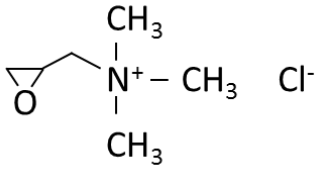

Fig. 3-1. Molecular structure of GTMAC

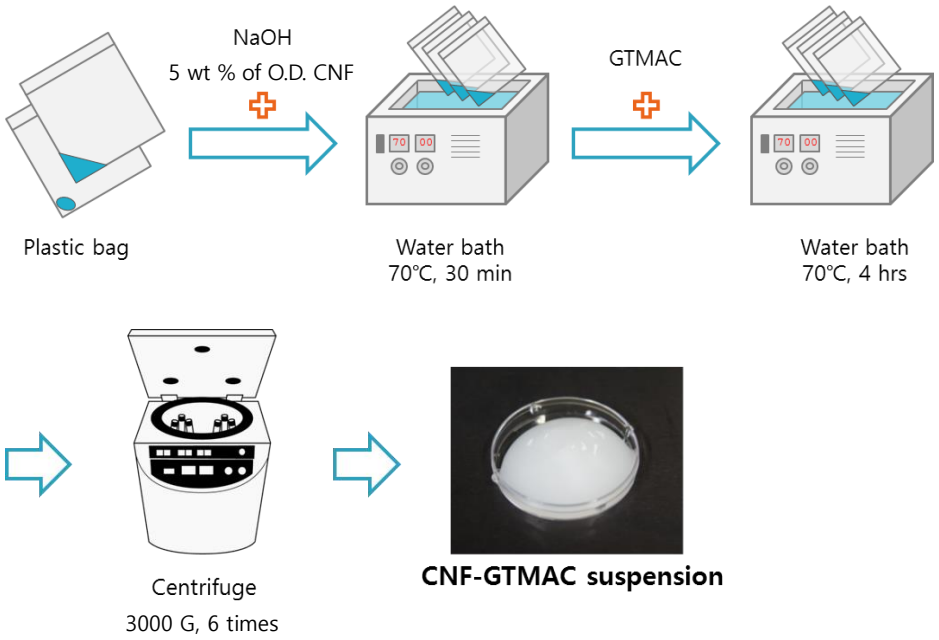

Fig. 3-2. Scheme of cationic modification process of CNF using GTMAC etherification

2.4. Characterization of cationic modified CNF

2.4.1. Zeta potential

The zeta potential of the CNF suspension was measured using a Nanosizer ZS (Malvern) based on the laser Doppler electrophoresis technique. A small amount of CNF suspension was diluted with deionized water and then injected into a folded capillary cell. The zeta potential was calculated by measuring the electrophoretic mobility using the Smoluchowski approximation. The temperature of the CNF suspension was held at 25 ℃ and the pH was about 6.

2.4.2. Nitrogen content measurement

To determine the amount of GTMAC grafted onto CNF, the nitrogen content of the CNF-GTMAC was measured. As in the sample preparation step for the FT-IR measurement in Chapter 2, CNF-GTMAC films were prepared. The nitrogen content of the CNF-GTMAC film was determined using an automatic Kjeldahl nitrogen analyzer (Kjeltec Auto 1035, Tecator AB).

3. Results and Discussion

3.1. Etherification of cellulose by GTMAC

The cationic modification of CNF was achieved through an etherification process involving the alkali-activated cellulose hydroxyl group and the epoxy group GTMAC. This reaction scheme is shown Fig. 3-3. By grafting GTMAC with a quaternary ammonium group, the negative surface charge of the CNF surface is converted to a cationic charge. However, two side reactions also arise: the hydrolysis of the GTMAC itself and the hydrolysis of the ether linkage of the cationic cellulose (Fig. 3-4).

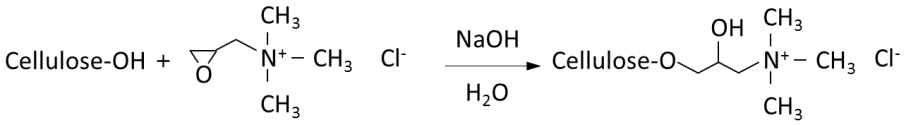

Fig. 3-3. Etherification of cellulose by GTMAC

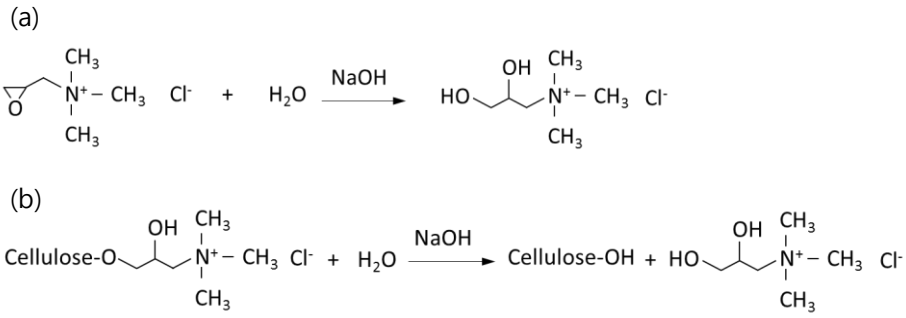

Fig. 3-4. Side reaction of cationic modification of CNF; (a): hydrolysis of GTMAC, (b): hydrolysis of ether linkage between GTMAC and cellulose

The cationic modification of CNF is carried out by means of esterification between the dissolved GTMAC molecules and the hydroxyl groups on the CNF surface. As the water content decreases, less water is available for the hydrolysis of GTMAC; as a result, the GTMAC is able to react with the alkali-activated cellulose (Zaman et al. 2012). That is, the water content of the reaction mixture is one of the most critical factors for the cationic modification of CNF. Based on the same principle, dry, semi-dry, and organic solvent reaction systems have been developed for the cationization of starches (Bendoritiene et al. 2006, Khalil et al. 2001), hemicellulose (Liu et al. 2011), and cellulose nanocrystal (Zaman et al. 2012).

In this research, the water in the CNF suspension was dewatered using pressurized dewatering equipment and the solids content of the resulting CNF was increased to 7.5 wt %. GTMAC with a 90 wt % solids content was used as cationization agent, and the consistency of the NaOH solution was 50 %. To investigate the effect of the water content of the reaction mixture on the cationization efficiency, the consistency of the CNF was controlled by adding deionized water to the concentrated CNF pad (7.5 wt %). The molar ratio of the GTMAC added to the AGU of CNF was 0.5. The reaction conditions are listed in Table 3-1. As described above, the effect of the water content of the reaction mixture on the cationic charge conversion of CNF was clearly observed, as shown in Fig. 3-5. At a low solids content of the reaction mixture (0.5 – 2 %), the zeta potential of the CNF did not change. As the solids content was increased from 2 % to 7.4 %, the zeta potential of CNF was converted to a positive charge, reaching a plateau at + 31 mV.

Fig. 3-6 shows the zeta potential of CNF treated with different amounts of GTMAC. The solids content of the CNF pads was 7.0 wt% in this case. The molar ratio of the GTMAC added to the AGU of CNF was varied from 0.05 to 0.3. As shown in Fig. 3-6, the conversion of the zeta potential of CNF to a positive charge was nearly proportional to the dosage of GTMAC in this range.

Table 3-1. Cationization reaction conditions with different solids content of starting CNF suspension or pad

Solids content of reaction mixture, %	0.8	1.5	3.0	4.5	6.0	7.4	8.8	9.7
Solids content of CNF suspension or pad, %	0.5	1.0	2.0	3.0	4.0	5.0	6.0	7.0
GTMAC to AGU ratio	0.5							
NaOH dosage, %	5							
Reaction temperature, ℃	70							
Reaction time, hrs	4							

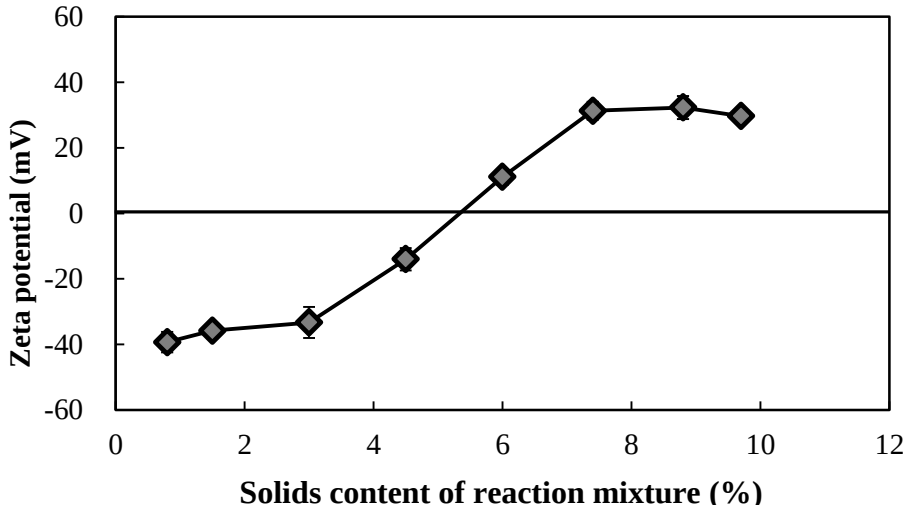

Fig. 3-5. Zeta potential of GTMAC-treated CNF according to solids content of reaction mixture

Table 3-2. Cationization reaction conditions with different amount of GTMAC

GTMAC to AGU of CNF ratio	0.05	0.10	0.15	0.20	0.25	0.30
Solids content of reaction mixture, %	7.6	7.9	8.2	8.5	8.8	9.1
Solids content of CNF pad, %	7.0					
NaOH dosage, %	5					
Reaction temperature, ℃	70					
Reaction time, hrs	4					

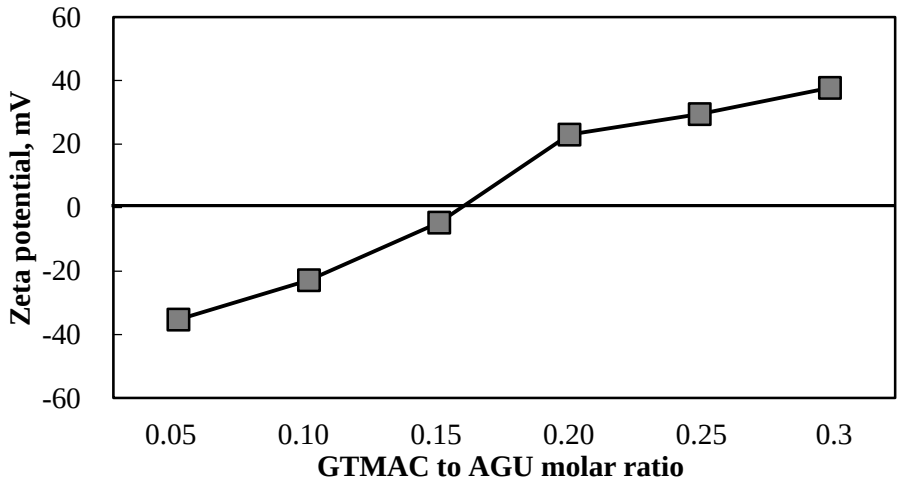

Fig. 3-6. Zeta potential of GTMAC-treated CNF according dosage of GTMAC

3.2. Degree of substitution and reaction efficiency

The degree of substitution (DS) of cationically modified CNF was defined as the number hydroxyl groups on each anhydroglucose unit of cellulose which are etherified by GTMAC (grafted GTMAC). Therefore, DS was derived as following Eq.(4-1).

$$Degree\ of\ substitution = \frac{n_{grafted\ GTMAC}}{n_{AGU}} \quad (4\text{-}1)$$

GTMAC molecule contains one nitrogen atom, therefore the quantity of GTMAC was measured by Kjeldahl analysis. The molar number of grafted GTMAC onto CNF was calculated as Eq.(4-2).

$$n_{grafted\ GTMAC} = \frac{w_{sample} \times N\%}{Aw_N} \quad (4\text{-}2)$$

Here w_{sample} is weight of sample (g), *N%* is the portion of nitrogen of CNF-GTMAC, and Aw_N is atomic weight of nitrogen, 14.007 (g/mol).

The molar number of AGU was calculated as Eq. (4-3) with the assumption that CNF consists of cellulose only.

$$n_{AGU} = \frac{W_{sample}(Aw_N - N\% \times Mw_{GTMAC})}{Aw_N \times Mw_{AGU}} \quad (4\text{-}3)$$

Here Mw_{GTMAC} is the molecular weight of GTMAC, 151.64 g/mol, and Mw_{AGU} is the molecular weight of AGU, 162.15 g/mol.

Therefore, Eq.(4-1) is derived as following Eq.(4-4).

$$Degree\ of\ substitution = \frac{N\% \times Mw_{AGU}}{Aw_N - N\% \times Mw_{GTMAC}} \quad (4\text{-}4)$$

The reaction efficiency (*% RE*) refers to the percentage of the initially added amount of GTMAC to the amount of GTMAC grafted onto CNF. The reaction efficiency was calculated by Eq. (4-4)

$$Reaction\ efficiency = \frac{n_{grafted\ GTMAC}}{n_{added\ GTMAC}} \times 100\ (\%) \quad (4\text{-}5)$$

Showing the same tendency with the change in the zeta potential, the degree of substitution (*DS*) and the reaction efficiency (*% RE*) were increased as the water content of the cationic reaction mixture was decreased (Fig. 3-7). On the other hand, when the solids content of the starting CNF pad was 7 wt %, the reaction efficiency remained at the same level (Fig. 3-8). The maximum value of the degree of substitution was 0.015 at a solids content of 9.7 wt % of the reaction mixture.

As shown in Fig. 3-8, the maximum reaction efficiency was 5.3 %; however, the reaction efficiency showed a slight decrease when the GTMAC-to-AGU ratio exceeded 0.20. The zeta potential of GTMAC exhibited a cationic charge at this dosage level; therefore, it appeared that the use of GTMAC on the hydroxyl groups of CNF was hindered by the electrostatic repulsive force.

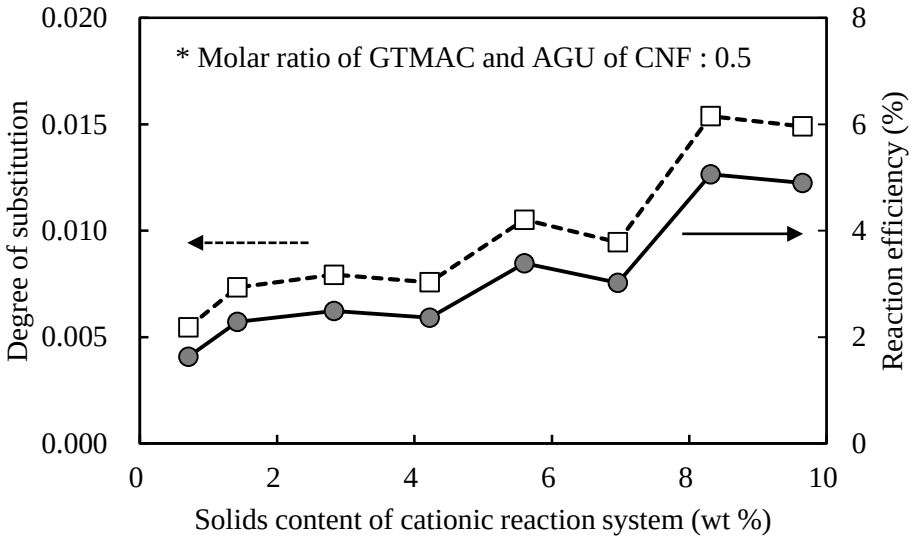

Fig. 3-7. Degree of substitution and reaction efficiency according to solids content of reaction system

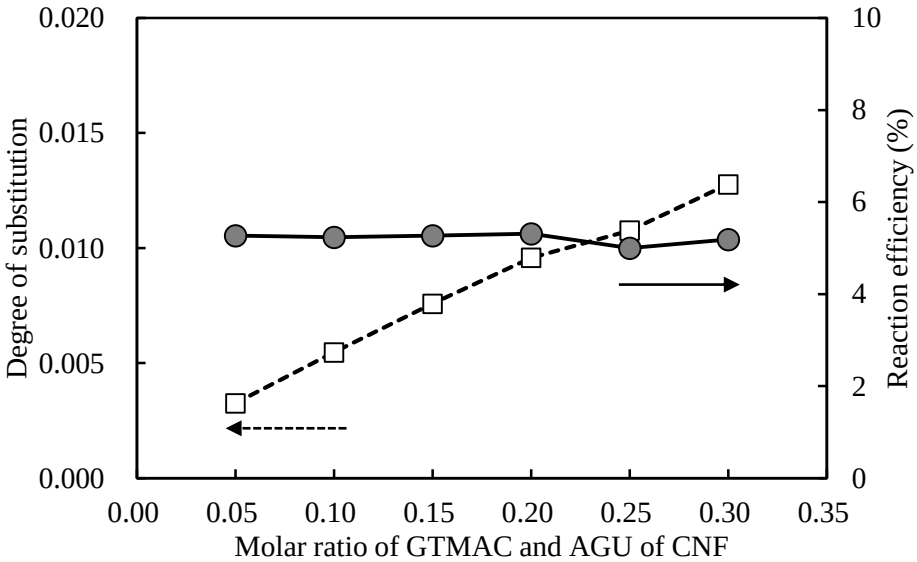

Fig. 3-8. Degree of substitution and reaction efficiency according to dosage of GTMAC

The degree of substitution and the reaction efficiency are rather low compared to previously reported instances of the cationic modification of cellulose nanomaterials, in which a semi-dry DMSO reaction system was used to reduce the water content of the reaction mixture (a maximum degree of substitution of 0.02, from Hasani et al. (2008) and a maximum reaction efficiency of 22% from Zaman et al. (2012)). As described above, the reaction of GTMAC with the alkali-activated hydroxyl groups of cellulose is in competition with the alkali hydrolysis of the GTMAC and the degradation of cationic cellulose. Compared to CNF, which is a suspended solid material, GTMAC is a water-soluble molecule, and the alkali hydrolysis of GTMAC is a more favorable reaction. As the water content of the reaction mixture is reduced, less water is associated with the hydrolysis of GTMAC and more GTMAC can be used in the etherification process. Therefore, the reaction efficiency and degree of substitution can be optimized by decreasing the water content of the reaction mixture. However, the extent of dewatering was limited due to the intrinsic hydrophilic nature of CNF. In an aqueous suspension, individual CNF fibers develop mechanical entanglement. As the solids content increases, CNF fibers become densified and the network structure is reinforced. When the consistency of the CNF suspension exceeds 7 wt%, the CNF pad becomes too densified for hand kneading of the reaction mixture. Therefore, the total solids content of the reaction mixture is limited to around 10 wt %. To increase the reaction efficiency and degree of substitution further, the water content of the reaction mixture can be reduced through the use of a polar organic solvent such as DMSO for reaction media (Ho et al. 2011) or with the use of dried cellulose as a raw material (Zaman et al. 2012). However, for the CNF suspension, these

methods require the use of an organic solvent and a solvent exchange process. The objective of this research is to prepare cationic CNF for a surface-charge-modified cross-linked CNF aerogel by an aqueous process. Therefore, the methods described above were not considered.

4. Summary

The surface charge of CNF was made positive through surface modification with glycidyltrimethylammonium chloride (GTMAC). In an etherification process, GTMAC was grafted onto the surface of CNF. Using the quaternary ammonium groups of GTMAC, the zeta potential of the cationic CNF was increased to +39.5 mV. The amount of grafted GTMAC was determined using the nitrogen content of the CNF-GTMAC and the degree of substitution was estimated.

It was found that the cationic reaction process was significantly affected by the water in the reaction mixture. As the water content was increased, the undesirable hydrolysis of GTMAC accelerated and less GTMAC was able to react with the hydroxyl group of cellulose. In this research, CNF was produced by a grinding treatment of pulp slurry, and the solids content was 2.0 wt %. When this CNF suspension was used as a starting material for a cationic modification process without a dehydration process, a charge conversion effect did not arise. The water in the CNF suspension could be dehydrated using a pressurized dehydrating device, and the zeta potential of CNF became positive. However, the dehydration of CNF was limited to a solids content of 7 wt % due to the tendency of CNF to form a strong fiber network structure. The maximum reaction efficiency reached 4.1 % due to the dehydration of the CNF suspension.

Chapter 4

Ion adsorption property of cross-linked cellulose nanofibrils aerogel

1. Introduction

One of potential application of the CNF aerogel is as a loading matrix for precious materials such as catalysts or drug chemicals due to its high specific surface area, strong mechanical properties and good biocompatibility (Sehaqui et al. 2010). As noted in the previous chapter, a cross-linked CNF aerogel with improved network stability in a wet state was prepared. The cross-linked CNF aerogel maintained its aerogel network structure in water with a shear condition; therefore, it can likely be applied to underwater applications.

Applications of CNF as a loading matrix for chemicals have been reported in previous studies. Dong et al. (2013) reported the loading of silver^{+} nanoparticles to a CNF suspension. Due to their positive charge, the silver nanoparticles were adsorbed onto the surface of the CNF by electrostatic attraction force, and strong gelation of the CNF was induced. Kolakovic et al. (2011) also reported the application of CNF films as a loading matrix for drug chemicals. They demonstrated that model active pharmaceutical ingredients (APIs) can be loaded onto CNF aerogel by a simple filtration method with a loading rate of 40%. Specifically, the drug release rate of the API-loaded CNF film was sustained for three months. Valo et al. (2013) also reported the application of CNF aerogel as a drug-delivery material. However, in their research, model chemicals were loaded by means of a simple mixing process with the CNF in a suspension state. Therefore, controlling the chemical loading rate was difficult and the loaded chemicals can be lost during the aerogel preparation process. In contrast, ionic chemicals can be loaded onto the cross-linked CNF aerogel by an ion-adsorption process. It was reported that

chemically modified cellulose materials exhibited good ion-adsorption performance. Karnitz et al. (2007) prepared succinic-acid-modified sugarcane bagasse, while de Melo et al. (2009) prepared maleic-anhydride-treated microcrystalline cellulose. In both studies, carboxylic moieties were grafted onto cellulose fibers and the anionic charge of the cellulose was enhanced by the added carboxyl groups. Those chemically modified fibrous cellulose samples exhibited superior cation exchange performance levels.

In this chapter, a negatively charged cross-linked CNF aerogel and a positively charged cross-linked CNF aerogel were prepared with CNF grafted with maleic acid and with CNF grafted with maleic acid and GTMAC, respectively. To investigate of ion-adsorption characteristics of these cross-linked CNF aerogels, metal cation and anion solutions were used. The effects of the contact time and the pH of the ion solution on the ion-adsorption characteristics of the cross-linked CNF aerogel as well as the theoretical adsorption capacities were determined by ion-adsorption experiments.

2. Materials and methods

2.1. Preparation of CNF

Commercial bleached eucalyptus kraft pulp was used as a raw material. Dried pulp sheets were dispersed in deionized water and were refined using a laboratory valley beater as a mechanical pretreatment. After 10 minutes of disintegration, the pulp slurry was beaten for 12 minutes and 30 seconds to obtain a freeness value of 450 mL CSF. The beaten pulp slurry was concentrated until its solids content was 2 wt %. The beaten fiber suspension was processed using a grinder (Super Masscollider MKCA6-3, Masuko Sanguo Co.). The pulp fibers were then passed through a gap between a static ceramic grinding stone and a rotating grinding stone revolving at 1,500 rpm. The gap was adjusted to -60 μm, with 40 passes. Prepared CNF suspension was dehydrated using pressurized dewatering equipment (Quro). A Whatman No. 2 filter paper was placed in the bottom of the cylinder as the filter media, after which approximately 100 g of the CNF suspension was transferred into the cylinder. Thereafter, the CNF suspension was pressed at 6 bar for 1 hour. As a result, a CNF pad was created with a solids content of about 7.5 wt%.

2.2. Cationic modification of CNF

For the cationic surface modification of CNF, glycidyltrimethyl-ammonium chloride (GTMAC) was used as a cationization agent. NaOH was used as a catalyst. These chemicals were obtained from Sigma-Aldrich and used without further purification. The dosage of GTMAC, which calculated as the

molar ratio of GTMAC and anhydroglucose unit (AGU) of cellulose, 0.5 molar ratio. The dosage of NaOH was 5 wt % of dry mass of CNF. After etherification treatment with GTMAC at 70 ℃ for 4 hours, cationic modified CNF (CNF-GTMAC) was produced.

2.3. Preparation of cross-linked CNF aerogels with negative and positive charge

For the cross-linking of CNF aerogel, maleic acid and sodium hypophosphite were used as cross-linking agent. As the starting materials, untreated CNF suspension and CNF-GTMAC suspension were used.

The maleic acid and hypophosphite were added to CNF and CNF-GTMAC suspension. The dosage of maleic acid, which calculated as the molar ratio of maleic acid to AGU of cellulose, was 10 molar ratio. After mixing for 30 min, the CNF suspension containing maleic and hypophosphite kept at 120 ℃ for 30 min using autoclave (MLS-3020, Sanyo Electric Co., Ltd.) for esterification between maleic acid and cellulose. The maleic acid-treated CNF (CNF-MA) and the maleic acid and GTMAC treated CNF (CNF-GTMAC-MA) suspensions were centrifuged at 3,000 G for 10 min. After centrifuging, CNFs were settled down and clear supernatants were removed. The CNF pad was re-dispersed in deionized water and additional centrifugal washing was carried out.

After centrifugal washing process, sodium hypophosphite was added to CNF-MA suspension with amount of 20 wt % based on oven-dried CNF-MA and CNF-GTMAC-MA. After that, total solids content of suspension was

adjusted to 3.5 wt % and transferred to polystyrene cuvette as a mold. Before rapid freezing, CNF hydrogels in cuvette were placed in refrigerator at 4 ℃ for overnight. Through this precooling step, fracture of frozen CNF suspension during rapid freezing can be minimized (Zheng et al. 2014). The precooled CNF hydrogels were rapidly frozen at -196 ℃ using liquid nitrogen and the frozen samples were subjected to freeze-drying using a freeze-dryer (FD8518, Ilshin Lab) for three days. The cold trap temperature was -80 ℃ and the vacuum level was maintained at 5 mmHg during the freeze-drying process. After three days of freeze-drying, rectangular CNF aerogels with a density of 36 kg/m^3 were prepared. Thereafter CNF aerogels were cured in convection oven to form cross-linking between cellulose fibrils. Curing temperature was 170 ℃ and time was 10 min. Cross-linked CNF aerogels were cut into cubes with size of 10 mm × 10 mm × 10 mm.

2.4. Measurement of zeta potential of CNF-MA and CNF-GTMAC-MA

Zeta potential of CNF suspension were measured using Nanosizer ZS (Malvern) based on the laser Doppler electrophoresis technique. Small amount of CNF suspension was diluted with deionized water and then was injected into folded capillary cell. The zeta potential was calculated by measuring the electrophoretic mobility using Smoluchwski's approximation. Temperature of CNF suspension was controlled at 25 ℃.

2.5. Evaluation of ion-adsorption properties

For the determination of the ion-adsorption performance of the cross-linked CNF aerogel, metal ions were used. For the cation adsorption of the negatively charged cross-linked CNF-MA aerogel, nickel nitrate ($Ni(NO_3)_2$), cobalt nitrate ($Co(NO_3)_2$), and cadmium nitrate ($Cd(NO_3)_2$) were used. For the anion adsorption of the positively charged cross-linked CNF-GTMAC-MA aerogel, potassium permanganate ($KMnO_4$) was used. These chemicals were purchased from Sigma-Aldrich. All solutions were prepared with deionized water.

The ion-adsorption process was carried out in a batch process, as follows. 25 mL of metal ion aqueous solutions were prepared in a conical tube, with different concentrations ranging from 0.1 to 5 mmol/L. A cubic cross-linked CNF aerogel was immerged into each metal ion solution. The oven-dry weight of a cubic cross-linked CNF aerogel sample was 0.036 g. During the ion-adsorption process, the conical tubes containing the ion solutions were shaken using a conical tube mixer. After the adsorption process, the CNF aerogels were removed from the metal ion solutions and the concentrations of the remaining metal ions in the solution were determined by ICP-OES (ICP-730 ES, Varian). The adsorption capacity (n_f) was calculated by the following equation (Eq. 4-1):

$$n_f = (n_i - n_s)/m \quad (4\text{-}1)$$

In this equation, ni is the initial molar numbers of ions, ns denotes the remaining molar number of ions in the solution, and m is the weight of the CNF aerogel.

3. Results and discussion

3.1. Chemical stability of cationically modified CNF during maleic acid esterification process

In the first step of the cross-linking treatment, the CNF is treated with maleic acid. To activate the esterification process, a high temperature is required. In this research, the CNF and maleic acid mixture is reacted at 120 ℃ for 30 min using an autoclave. However, to prepare the positively charged cross-linked CNF aerogel, the chemical stability of the cationically modified CNF should be ensured. Because cationically modified cellulose can be degraded through the hydrolysis of the ether linkage, particularly in an alkaline condition, the chemical stability of the cationically modified CNF in this study was assessed

GTMAC-treated CNF (CNF-GTMAC) suspensions were diluted to 0.1 wt%. The pH of the CNF-GTMAC suspension was adjusted from 3 to 11 using a 0.1 N NaOH and HCl solution. Then, these suspensions were kept at 120 ℃ for 0.5, 3.5, and 6.5 hours using an autoclave. The zeta potential of CNF-GTMAC after the heat treatment is shown in Fig. 4-1. In the alkaline and high-temperature condition, the zeta potential of CNF-GTMAC was maintained for 30 min. However, it decreased after 3.5 hours of reaction.

Because maleic acid is added to the CNF suspension with a high concentration during the esterification process, an acidic condition with a pH of 1 is generated. In addition, the esterification process was carried out for 30 min; therefore, the ether linkage of CNF-GTMAC is maintained during the

maleic-acid esterification process.

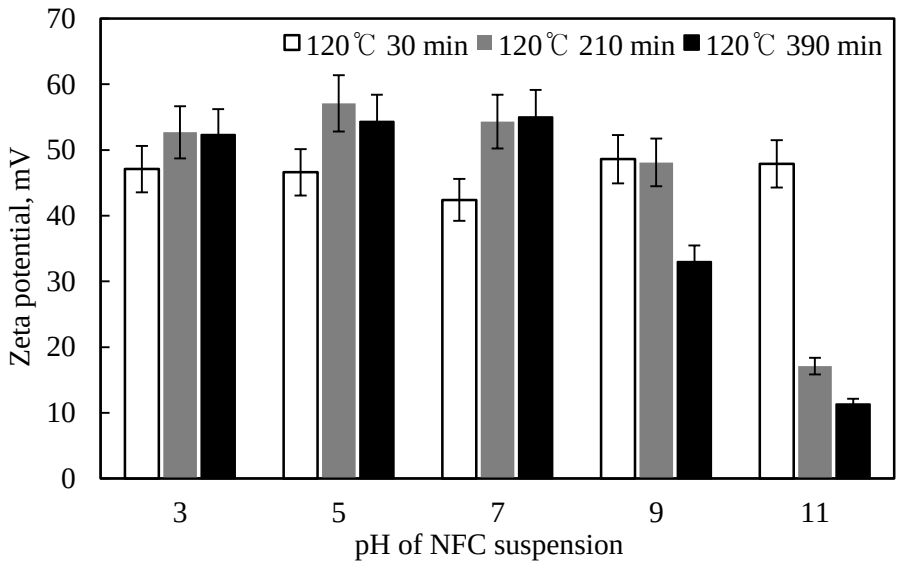

Fig. 4-1. Zeta potential of CNF-GTMAC after heat treatment at different pH

3.2. Zeta potential of CNF-MA and CNF-GTMAC-MA

In order to investigate the effect of the pH on the surface charge of the cross-linked CNF aerogel, the zeta potential values of CNF-MA and CNF-GTMAC-MA were measured. The pH of the CNF suspension was adjusted with a 0.1N NaOH and 0.1 N HCl solution, but the ionic strength of the suspension increased sharply at pH levels of 3 to 11 with the addition of the NaOH and HCl. The zeta potential is affected by the ionic strength of aqueous media due

to the compaction of the electric double layer at the higher ion concentration. Therefore, the NaCl solution was added to the CNF suspensions in order to equalize the ionic strength in this study. The conductivity levels of the CNF suspensions were adjusted to 0.9 ± 0.1 mS/cm for the pH range of 3 – 11, as shown in Fig. 4-3.

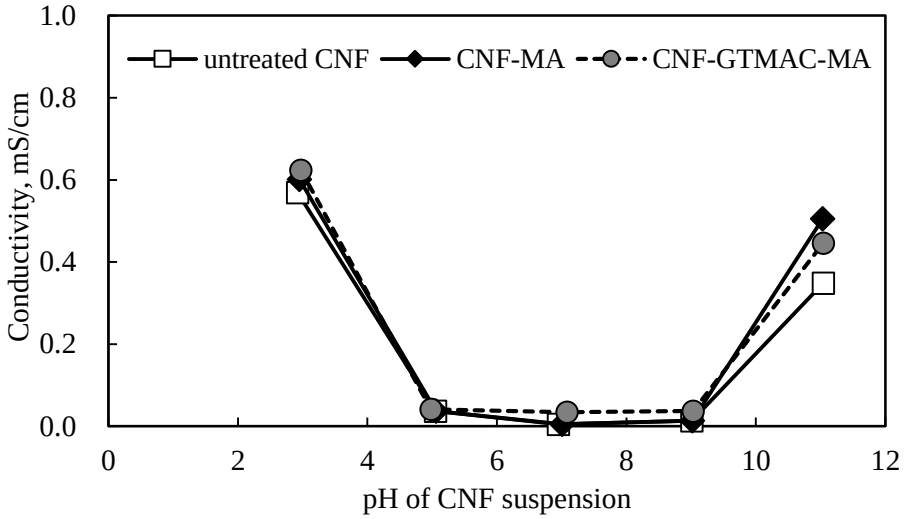

Fig. 4-2. Ionic strength of pH-adjusted CNF suspensions without NaCl addition

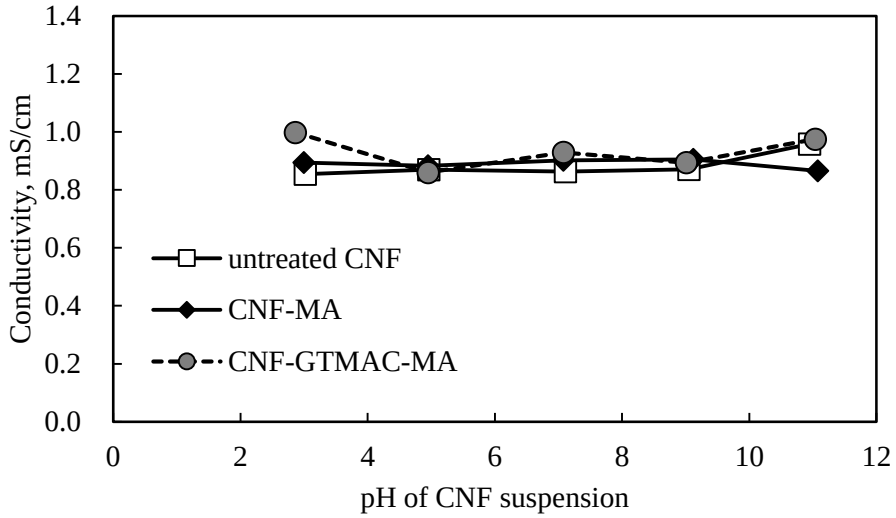

Fig. 4-3. Ionic strength of pH-adjusted CNF suspensions with NaCl addition

The changes in the zeta potentials of CNF-MA and CNF-GTMAC-MA according to the pH of the suspension are shown in Fig. 4-4. CNF-GTMAC-MA showed the highest positive charge at pH 3, and the surface charge decreased as the pH was increased. At pH 12, the surface charge of CNF-GTMAC-MA was almost neutral. In contrast, CNF-MA showed a higher negative charge in an alkaline condition above pH 7.

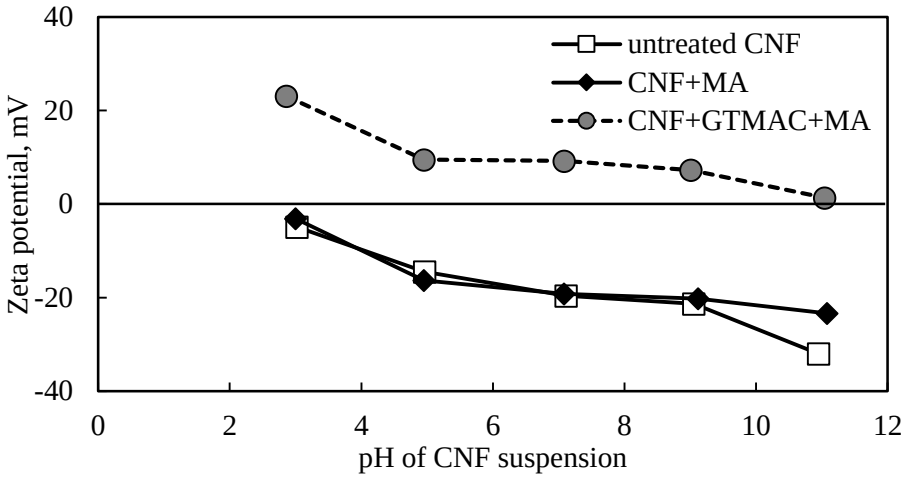

Fig. 4-4. Zeta potential of CNF with pH 3 – 11

The cross-linking process of CNF using maleic acid and sodium hypophosphite consisted of two reactions: the grafting of maleic acid onto cellulose and the cross-linked formation of grafted maleic acid through a reaction between maleic acid and hypophosphite. However, the formation of cross-linking between the maleic acid and the hypophosphite occurred in a solid state after the free-drying of the CNF aerogel. Therefore, some of the maleic acid was able to react with hypophosphite, while the rest of the maleic acid remained in the cellulose. As a result, the cross-linked CNF aerogel contains free carboxylic acid groups on the surface of the CNF, as in the scheme shown in Fig. 4-6. For the cationic cross-linked CNF aerogel, carboxylic groups also exist in addition to the quaternary ammonium groups of GTMAC. Carboxylic acid is a weak acid, and its dissociation into carboxyl anions is affected by the pH. That is, the presence of carboxylic groups means that the surface charge of the cross-linked CNF is affected by the pH of the aqueous media, i.e., both the positively (CNF-GTMAC-MA) and the negatively (CNF-MA) surface-charged aerogel.

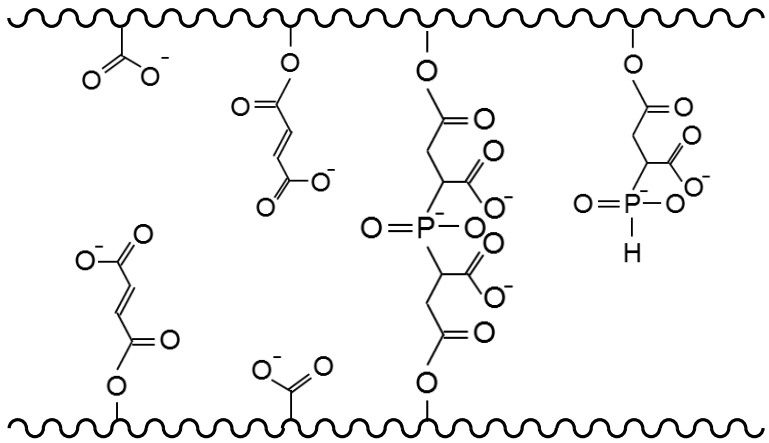

Fig. 4-5. Scheme for the molecular structure of cross-linked CNF-MA aerogel at alkaline condition

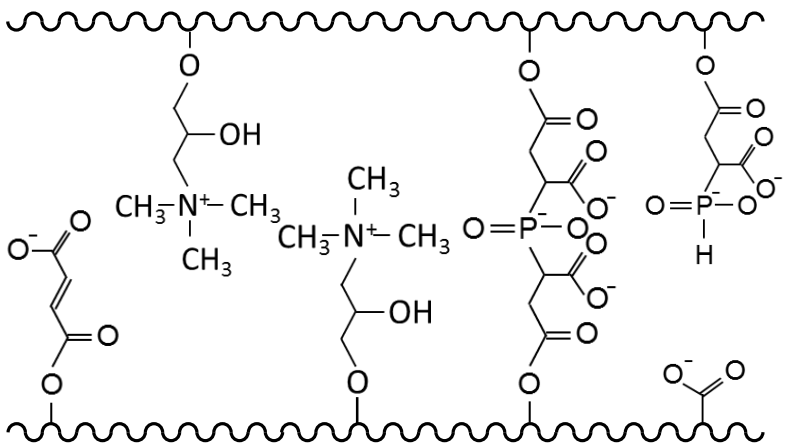

Fig. 4-6. Scheme for the molecular structure of cross-linked CNF-GTMAC-MA aerogel at alkaline condition

3.3. Effect of pH of solution on adsorption

As mentioned previously, the surface charge of the cross-linked CNF is affected by the pH of the aqueous media. Therefore, it is expected that the adsorption of metal ions from an aqueous solution is dependent on the pH. An experiment to assess the adsorption performance of the cross-linked CNF aerogel was carried out with 1 mM of metal ion solutions with different pH conditions ranging from 3 to 11. A nickel nitrate solution for the negatively charged CNF aerogel and a potassium permanganate solution for the positively charged CNF aerogel were used as the metal solutions, respectively. The adsorption time was 3 hours. The adsorption capacities (n_f) after 3 hours of ion exchange are presented in Fig. 4-6 and 4-7. The negatively charged CNF aerogel showed the maximum adsorption of Ni^{2+} at a pH of 11 and the positively charged CNF aerogel showed the maximum adsorption of MnO_4^- at a pH of 3, corresponding to the result of the surface charge.

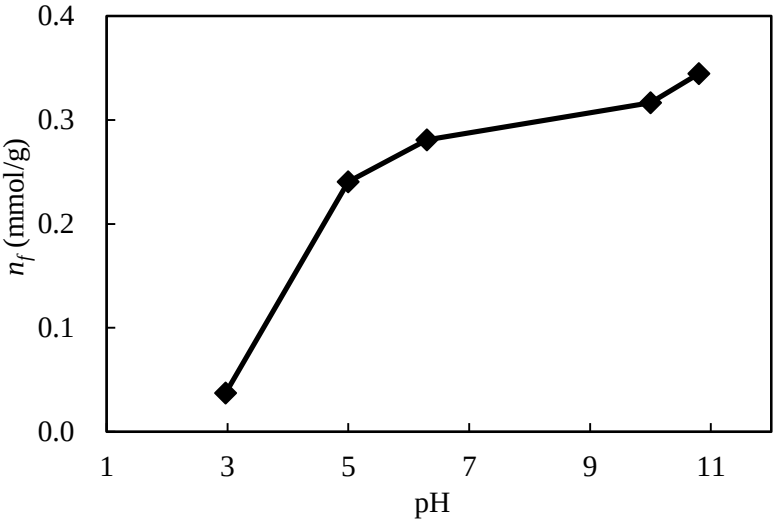

Fig. 4-7. Nickel ion adsorption of negative charged cross-linked CNF aerogel depend on the pH

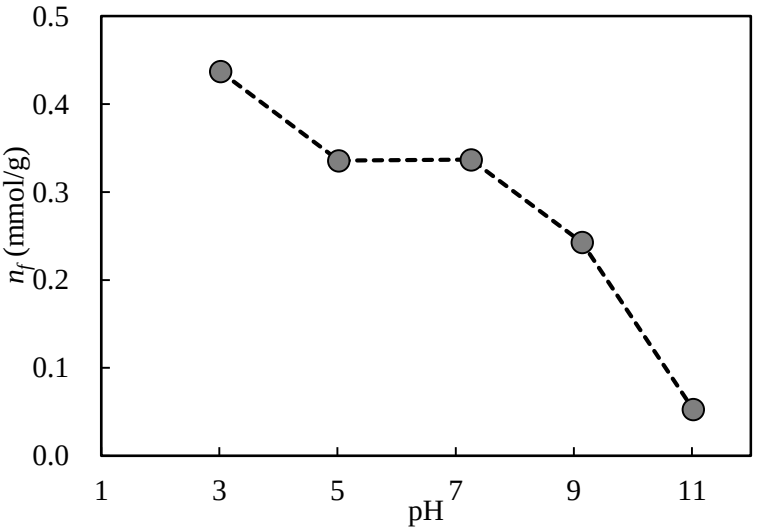

Fig. 4-8. Permanganate ion adsorption of positive charged cross-linked CNF aerogel depend on the pH

3.4. Contact time for adsorption equilibrium

An experiment to assess the adsorption kinetics was performed in a batch process while varying the adsorption time from 10 minutes to 3 hours. As the adsorbate, 1 mM each of nickel nitrate and potassium permanganate solutions were used. The pH was adjusted to 11 for the nickel nitrate solution and 3 for the potassium permanganate solution.

Fig. 4-9 and Fig. 4-10 show the kinetics of adsorption onto the negatively and positively cross-linked CNF aerogels. These figures show that a state of adsorption equilibrium was reached after 60 minutes for both the negatively charged and positively charged aerogels.

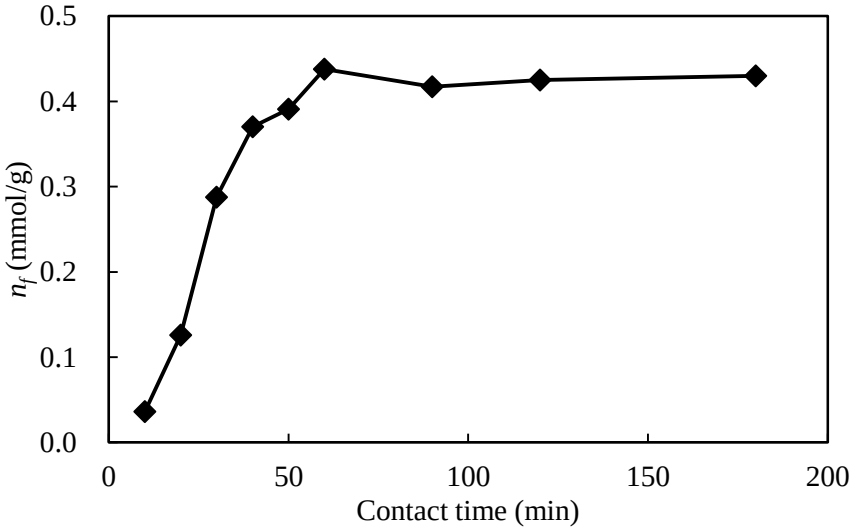

Fig. 4-9. Nickel ion adsorption of negative charged cross-linked CNF aerogel with contact time

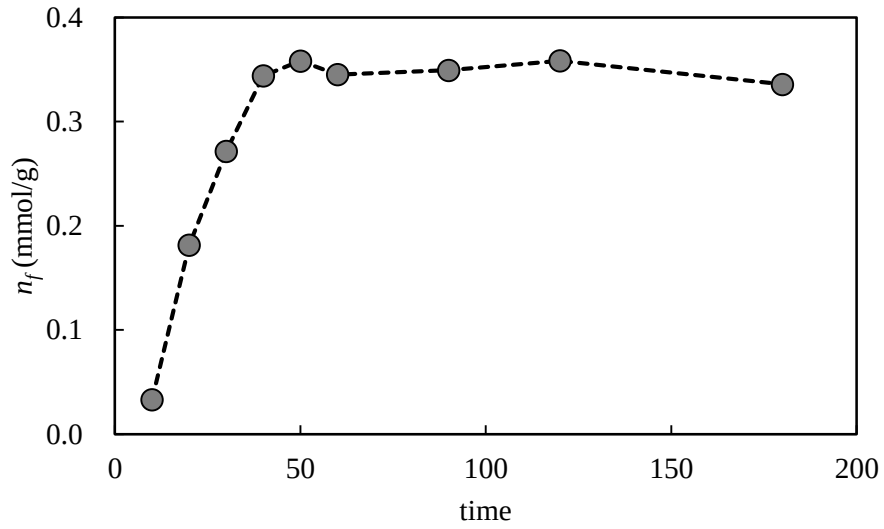

Fig. 4-10. Permanganate ion adsorption of positive charged cross-linked CNF aerogel with contact time

3.5. Maximum adsorption capacity of cross-linked CNF aerogel

To study the adsorption isotherm of the negatively charged CNF aerogel, cobalt, cadmium, and nickel ion solutions were prepared. For the positively charged CNF aerogel, permanganate and dichromate anions were used. In both the cation and anion solutions, the concentrations were varied from 0.1 to 5 mmol/L. After 3 hours of adsorption, equilibrium adsorption isotherm data for the remaining metal ion concentration were obtained. As a result, the adsorption isotherm, a function of the adsorption capacity for the concentration of the remaining metal ion solution, was derived.

To evaluate the adsorption performance of the cross-linked CNF aerogel, the Langmuir adsorption model (de Melo et al. 2009, Abo-Farha et al. 2009) was employed. According to the Langmuir adsorption model, it is assumed that each of the adsorbed ions is held by a definite point of attachment on the surface. Given this assumption, the maximum adsorption capacity corresponding to complete monolayer coverage is estimated (Abo-Farha et al. 2009). During the adsorption process at the liquid/solid interface, a state of dynamic equilibrium exists between the solved ions in the liquid and the ions adsorbed onto the solid. Thus, the ratio between the number of moles in the solution and that of the ions adsorbed on the CNF surface is expressed in terms of the Langmuir isotherm, as Eq. (4-2).

$$\frac{C_S}{n_f} = \frac{C_S}{n^S} + \frac{1}{n^S b} \quad (4\text{-}2)$$

Here, C_s (mol/L) is the concentration of the remaining metal ions in the solution in an equilibrium state. From the linearized adsorption isotherm, where C_s/N_f is considered to be a function of C_s, the remaining parameters n_s (mol/g; the maximum amount of adsorbed metal ions per mass of CNF aerogel) and b (L/mol, constant value) were determined.

The linearized Langmuir adsorptions of the metal ions are shown in Fig. 4-11. From the Langmuir adsorption isotherm, the adsorption parameters are listed in Table 4-1.

The n_s value, the maximum ion absorption capacity of the negatively charged cross-linked CNF aerogel, was 0.79 mmol/g for the Ni^{2+} ion, while that in the positively charged case was 0.62 mmol/g for MnO_4^-. These values were rather low compared to reported results of chemically modified micro-particular cellulose absorbent materials (1.8 – 2.5 mmol/g by de Melo et al. in 2009 and 1.74-2.78 mmol/g according to Karnitz et al. in 2007). However, they are appreciably higher than a commercially available strong acid ion-exchange resin (0.05 – 0.1 mmol/g by Abo-Farha et al. 2009).

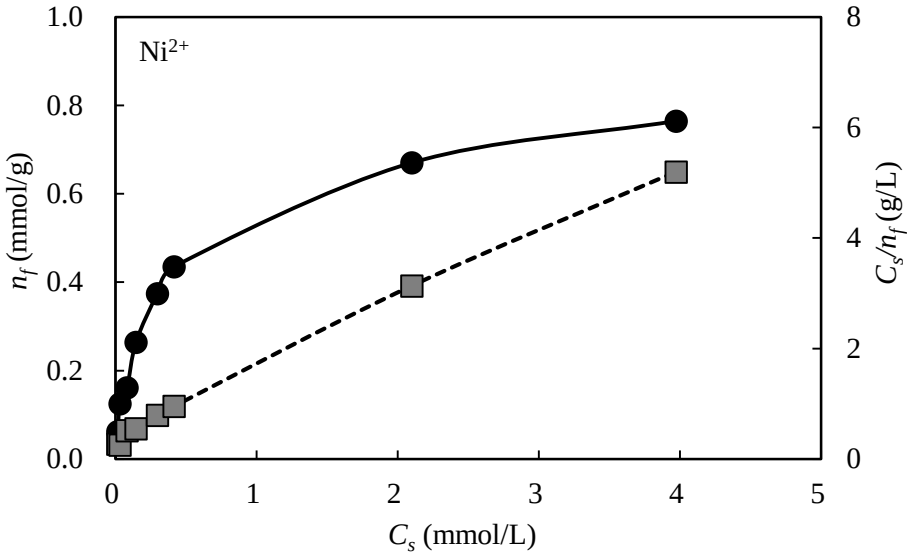

Fig. 4-11. Adsorption isotherms of negative charged cross-linked CNF aerogel (metal ion: Ni^{2+})

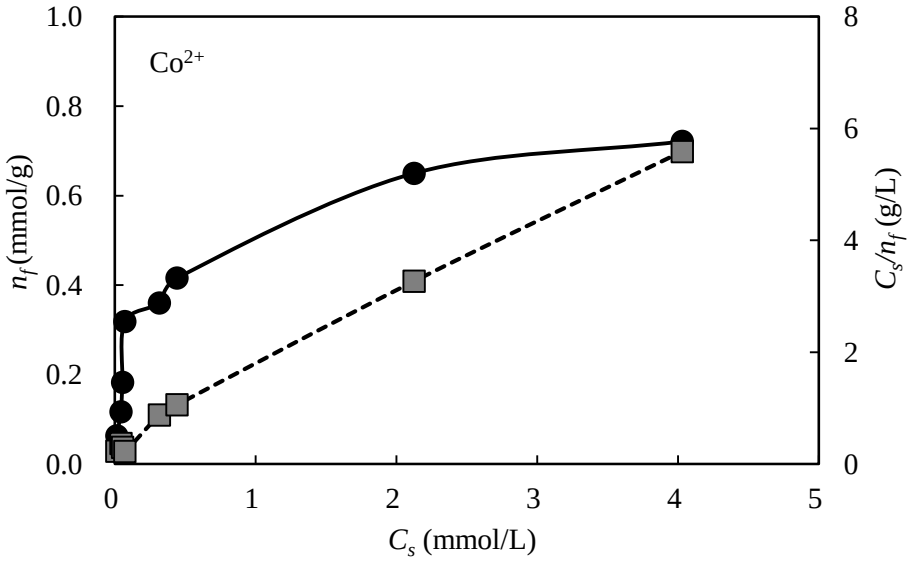

Fig. 4-12. Adsorption isotherms of negative charged cross-linked CNF aerogel (metal ion: Co^{2+})

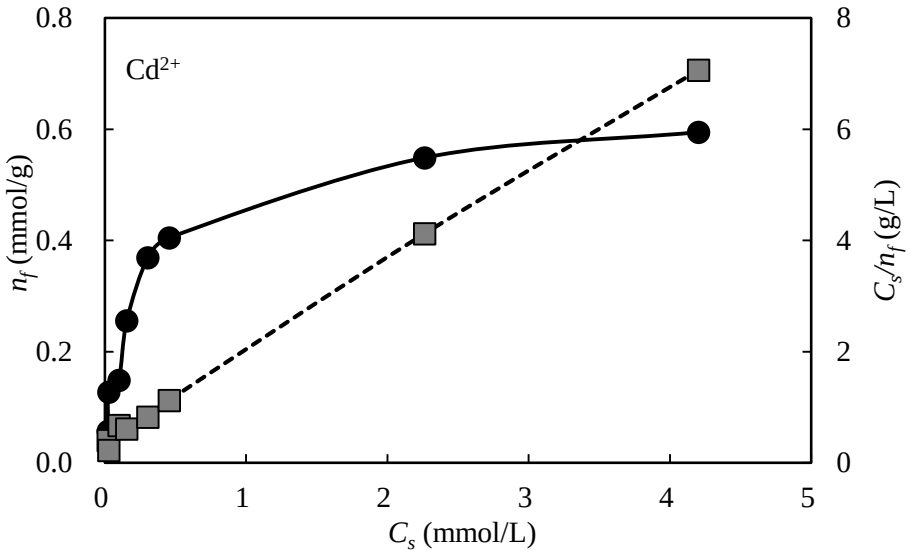

Fig. 4-13. Adsorption isotherms of negative charged cross-linked CNF aerogel (metal ion: Cd^{2+})

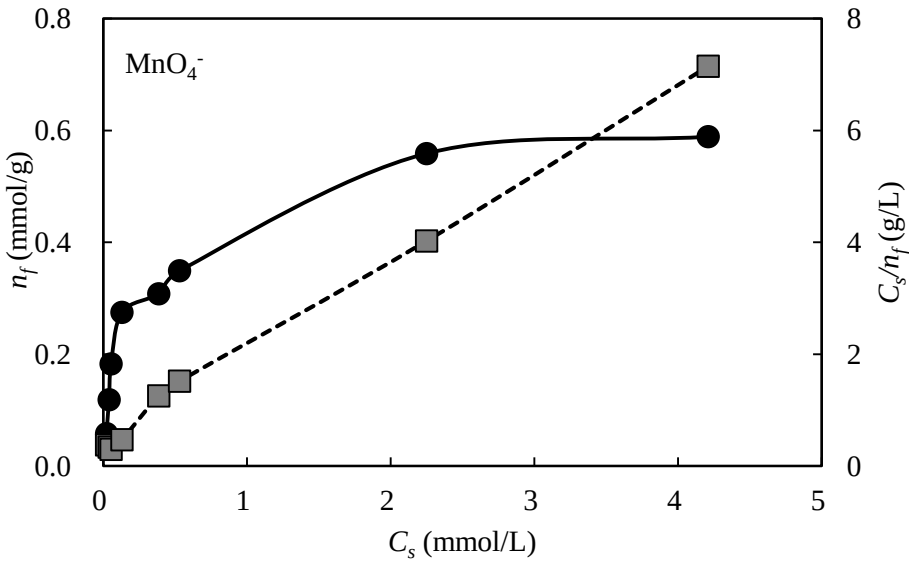

Fig. 4-14. Adsorption isotherms of positive charged cross-linked CNF aerogel (metal ion: MnO_4^-)

Table 4-1. The Langmuir adsorption isotherm parameters

Metal ion	n_s(mmol/g)	b(L/mol)	R^2
Ni^{2+}	0.79	3.46	0.9953
Co^{2+}	0.75	4.33	0.9982
Cd^{2+}	0.62	4.41	0.9954
MnO_4^-	0.618	4.16	0.9953

4. Summary

In this study, negative surface-charged and positive surface-charged cross-linked CNF aerogels were prepared with CNF grafted by maleic acid (CNF-MA) and with CNF grafted with maleic acid and GTMAC (CNF-GTMAC-MA), respectively. The zeta potentials of CNF-MA and CNF-GTMAC-MA were affected by the pH of the aqueous media. CNF-MA showed a weak negative charge at pH 3, and the negative charge became stronger as the pH was increased due to the dissociation of the carboxyl groups. On the other hand, the zeta potential of CNF-GTMAC-MA exhibited the strongest positive charge at a pH of 3, though the strength decreased with an increase in the pH.

The ion adsorption of cross-linked CNF aerogels was influenced by the pH due to the surface charge. The negatively charged cross-linked CNF aerogel showed the highest adsorption performance of a nickel cation at pH 11, whereas the positively charged cross-linked CNF aerogel showed the highest adsorption of a permanganate anion at pH 3.

Both cross-linked CNF aerogels reached an equilibrium adsorption state after 1 hour. Isotherm adsorption was carried out, and the theoretical maximum adsorption performance levels of the cross-linked CNF aerogels were determined using the Langmuir adsorption model. The maximum ion-adsorption capacity of the negatively charged cross-linked CNF aerogel was 0.79 mmol/g for the nickel cation while that of the positively charged cross-linked aerogel was 0.62 mmol/g for the permanganate anion.

Chapter 5

Overall conclusions

CNF aerogels are fascinating materials with the high porosity, ultra-lightweight, high specific surface area characteristics. Also, as a member of cellulose based derivatives, it possesses biodegradability, biocompatibility, availability, renewability, and possibility for various chemical modification. Moreover, CNF aerogels are produced with environmentally-friendly process compared to conventional aerogel made with inorganic materials or dissolved cellulose which requires multiple solvent-exchange stages and considerable amount of energy as well. However, the network structure of CNF aerogels relies on interfibrillar hydrogen bonds between adjacent individual fibers. As a result, the network structure of CNF aerogels is easily destroyed by absorbed water. This weakness of the wet strength limits the wider applicability of CNF aerogels.

In this research cross-linked CNF aerogel was prepared with maleic acid and sodium hypophosphite. The cross-linking reaction consisted of two steps: 1) the esterification of CNF with maleic acid, and 2) the formation of a cellulose cross-linkage by a reaction between maleic acid and hypophosphite. Prepared cross-linked CNF aerogel exhibited ultralight and highly porous internal structure. Also it showed improved network stability toward moisture and water absorbency.

The cross-linked CNF aerogel showed shape-recovery characteristics in a wet state. After compression in a wet state, the cross-linked CNF aerogel recovered its original shape within a few seconds, while the untreated CNF aerogel collapsed and did not recover its original shape. The shape-recovery performance was evaluated using the springiness value from a TPA test. The

springiness value of the cross-linked CNF aerogel was 0.78, while that of the untreated aerogel was only 0.33. The shape-recovery characteristic of the cross-linked CNF aerogel was explained in terms of the interaction between the absorbed water and the CNF nanopaper.

Typically, cellulose fibers have a negative charge due to the carboxyl group in their chemical composition. The anionic charge of cellulose fiber surface repels other anionic materials by electrostatic repulsive force. In this research, the surface charge property of the CNF was modified to cationic charge to adjust the interaction of the CNF with ionic materials. Glycidyltrimethylammonium chloride (GTMAC) was used as a cationic modification agent. The epoxy group of GTMAC reacted with the hydroxyl group of cellulose and formed an ether linkage. GTMAC-grafted CNF exhibited a positive charge of + 39.5 mV due to the quaternary ammonium group of GTMAC.

It was found that the cationic reaction process was significantly affected by the water in the reaction mixture. The solids content of CNF was 2.0 wt %, because it produced by grinding treatment of pulp slurry. When the CNF suspension was used as a starting material for a cationic modification process without a dewatering process, GTMAC treatment had no effect on the cationic modification of CNF. As the solids content of GTMAC treatment mixture was increased using pressurized dewatering equipment, surface charge of GTMAC treated CNF modified toward positive. However, the dehydration of CNF was limited to a solids content of 7 wt % due to the tendency of CNF to form a strong fiber network structure. The maximum value of degree of substitution

and reaction efficiency reached 0.015 and 5.3 %, respectively.

The cross-linked CNF aerogel exhibited negative surface charge because of the carboxyl groups of cellulose and grafted maleic acid. In contrast, the cross-linked CNF aerogel with positive surface charge was prepared using the cationically modified CNF as a starting material. The zeta potentials of maleic acid treated CNF (CNF-MA) and maleic acid and GTMAC treated CNF (CNF-GTMAC-MA) were affected by the pH of the aqueous media. CNF-MA showed a weak negative charge at pH 3, and the negative charge became stronger as the pH was increased due to the dissociation of the carboxyl groups. On the other hand, the zeta potential of CNF-GTMAC-MA exhibited the strongest positive charge at a pH of 3, though the strength decreased with an increase in the pH.

The ion adsorption of cross-linked CNF aerogels was influenced by the pH due to the surface charge. The negatively charged cross-linked CNF aerogel showed the highest adsorption performance of a nickel cation at pH 11, whereas the positively charged cross-linked CNF aerogel showed the highest adsorption of a permanganate anion at pH 3.

Both cross-linked CNF aerogels reached an equilibrium adsorption state after 1 hour. Isotherm adsorption was carried out, and the theoretical maximum adsorption performance levels of the cross-linked CNF aerogels were determined using the Langmuir adsorption model. The maximum ion-adsorption capacity of the negatively charged cross-linked CNF aerogel was 0.79 mmol/g for the nickel cation while that of the positively charged cross-linked aerogel was 0.62 mmol/g for the permanganate anion.

The weak network structure toward aqueous condition is one of the main disadvantage of CNF aerogel. In this research, it was shown that this limitation of CNF aerogel is able to be overcome by cross-linking treatment with maleic acid and sodium hypophosphite. In addition, the cross-linked CNF aerogel exhibited water absorbency and shape recovery properties. Also the surface charge of the cross-linked CNF aerogel was modified and showed good ion adsorption capacities. Therefore, a wider range of potential applications of CNF aerogel is expected through these features, such as a loading matrix for catalysts or drug chemicals for aqueous conditions.

References

Abbott, A. P., Bell, T. J., Handa, S., and Stoddart, B., Cationic functionalization of cellulose using a choline based ionic liquid analoge, Green Chem. 8:784-786 (2006)

Abo-Farha, S. A., Abdel-Aal, A. Y., Ashour, I. A., and Garamon, S. E., Removal of some heavy metal cations by synthetic resin purolite C100, Journal of Hazardous Materials 169:190-194 (2009)

Alemdar, A., and Sain, M., Isolation and characterization of nanofibers from agricultural residues-wheat sraw and soy hulls. Bioresour. Technol. 99(6):1664-1671 (2008)

Aulin, C., Netrval, J, Wågberg, L., and Lindström, T., Aerogels from nanofibrillated cellulose with tunable oleophobicity, Soft Matter 6(14):3298-3305 (2010)

Andresen, M., Johansson, L., Tanem, B., and Stenius, P., Properties and characterization of hydrophobized microfibrillated cellulose, Cellulose 13(6):665-677 (2007)

Aulin, M., Johansson, L. S., Tanem, B. S., and Stenius, P., Properties and characterization of hydrophobized microfibrillated cellulose, Cellulose 13(6):665-677 (2009)

Bendoraitiene, J., Kavaliauskaite, R., Klimaviciute, R., and Zemaitaitis, A., Peculiarities of starch cationization with glycidyltrimethylammonium chloride. Starch 58(12): 623–631 (2006)

Brodin, F. W., Lund, K., Brelid, H., and Theliander, H., Reinforced absorbent material: a cellulosic composite of TEMPO-oxidized MFC and CTMP fibres, Cellulose 19(4):1413-1423 (2012)

Cai, J., Liu, S., Feng, J., Kimura, S., Wada, M., Kuga, S., and Zhang, L., Cellulose–silica nanocomposite aerogels by in situ formation of silica in cellulose gel, Angewandte Chemie 51(9):2076-2079 (2012)

Cervin, N. T., Aulin, C., Lasson, P. T., and Wågberg, L., Ultra porous nanocellulose aerogels as separation medium for mixtures of oil/water liquids, Cellulose 9(2):401-410 (2012)

Ciolacu, D., Ciolacu, F., and Popa, V. I., Amorphous cellulose – structure and characterization, Cellulose Chem. Technol. 45(1-2):13-21 (2011).

Chakraborty, A., Sain, M., and Kortschot, M., Cellulose microfibres: A novel method of preparation using high shear refining and cryocrushing, Holzforschung 60(1):53-58 (2005)

Chen, W., Haipeng, Y., Qing, L., Yixing, L., and Jian L., Ultralight and highly flexible aerogels with long cellulose I nanofibers, Soft Matter 7(21)10360-10368 (2011)

Chen, W., Lickfield, G. C., and Yang, C. Q., Molecular modeling of cellulose in amorphous state. Part I: model building and plastic deformation study, Polymer 45(3):1063-1071 (2004)

Cho, S. H., Kim, R., Park, J. J., and Lee, M. C., Durable press finishing of silk/cotton fabrics with BTCA (3) – the stydy of ester crosslinkages of silk/cotton fabrics treated with BTCA by FT-IR spectroscopy, Journal of Korean Society of Dyers and Finishers, 15(4):17-23 (2003)

de Melo, J. C. P., da Silva Filho, E. C., Santana, S. A. A., and Airoldi, C., Maleic anhydride incorporated onto cellulose and thermodynamics of cation-exchange process at the solid/liquid interface, Colloids and Surfaces A, 346(1-3):138-145 (2009)

Dong H, Snyder JF, Tran DT, Leadore JL. Hydrogel, aerogel and film of cellulose nanofibrils functionalized with silver nanoparticles. Carbohydrate Polymers 95:760-767 (2013)

Duchemin, B. J. C., Staiger, M. P., Tucker, N., and Newman, R. H., Aerocellulose based on all-cellulose composites, J. Appl. Polym. Sci. 115(1):216-221 (2010)

Dufresne, A., Cavaillé, J. Y., and Helbert, W., Thermoplastic nanocomposites filled with wheat straw cellulose whiskers. Part II: effect of processing and modeling, Polym. Composites 18(2):198–210 (1997)

Eriksen, Ø., Syverud, K., and Gregersen, Ø., The use of microfibrillated cellulose produced from kraft pulp as strength enhancer in TMP paper, Nord. Pulp Pap. Res. J. 23(3):299-304 (2008)

Gavillon, R., and Budtova, T., Aerocellulose: new highly porous cellulose prepared from cellulose-NaOH aqueous solutions, Biomacromolecules 9(1):269-277 (2008)

Goussé, C., Chanzy, H., Cerrada, M.L., and Fleury, E., Surface silylation of cellulose microfibrils: Preparation and rheological properties, Polymer 45(5):1569-1575 (2004)

Habibi, Y., Lucia, L. A., and Rojas, O. J., Cellulose nanocrystals: chemistry, self-assembly, and applications, Chem. Rev. 110(6):3479-3500 (2010)

Hasani, M., Cranston, E. D., Westman, G., and Gray, D. G., Cationic surface functionalization of cellulose nanocrystals, Soft Matter, 4:2238-2244 (2008)

Heath, L., and Thielemans, W., Cellulose nanowhisker aerogels, Green Chemistry 12(8):1448-1453 (2010)

Heiskanen, I., Backfolk, K., Vehviläinen, M., Kamppuri, T., and Nousiainen, P., Process for producing mucrofibrillated cellulose, European patent 2011004301, 28 June 2012

Henriksson, M., Henriksson, G., Berglund, L. A., and Lindstöm, T., An environmentally friendly method for enzyme-assisted preparation of microfibrillated cellulose (MFC) nanofibers, Eur. Polym. J. 43(8):3434-3441 (2007)

Herrick, F. W., Casebier, R. L., Hamilton, J. K., and Sandberg, K. R., Microfibrillated cellulose: morphology and accessibility, (1983) J. Appl. Polym. Sci. Appl. Polym. Symp. 37:797-813 (1983)

Hirota, M., Tamura, M., Saito, T., and Isogai, A., water dispersion of cellulose II nanocrystals prepared by TEMPO-mediated oxidation of mercerized cellulose at pH 4.8, Cellulose 17(2):279-288 (2009)

Ho, T. T. T., Zimmermann, T., Hauert, R., and Caseri, W., Preparation and characterization of cationic nanofibrillated cellulose from etherification and high-shear disintegration process, Cellulose 18(6):1391-1406 (2011)

Hult, E.-L., Iotti, M., and Lenes, M., Efficient approach to high barrier packaging using microfibrillar cellulose and shellac. Cellulose, 17(3), 575–586 (2010)

Husing, N., Schubert, U. Aerogels–airy materials: chemistry, structure, and properties. Angewandte Chemie International Edition 37:22–45 (1988)

Iwamoto, S., Nakagaito, A. N., Yano, H., and Nogi, M., Optically transparent composites reinforced with plant fiber-based nanofibers, Appl. Phys. A (2005)

Iwamoto, S., Nakagaito, A. N., and Yano, H., Nano-fibrillation of pulp fibers for the processing of transparent nanocomposites, Appl. phys. A 89(2):461-466 (2007)

Isogai, A., and Atalla, R. H., Dissolution of cellulose in aqueous NaOH solution, Cellulose 5(4):309-319 (1998)

Isogai, T., Saito, T., and Isogai, A., Wood cellulose nanofibrils prepared by TEMPO electro-mediated oxidation, Cellulose 18(2):421-431 (2011a)

Jin, H., Kettunen, M., Laiho, A., Pynnönen, H., Paltakari, J., Marmur, A., Ik kala, O., and Ras, R. H. A., Superhydrophobic and superoleophobic nanocellulose aerogel membranes as bioinspired cargo carriers on water and oil, Langmuir 27(5):1930-1934 (2011b)

Jo, J., Shin, J., Kim, W., So, K., Im, H., Seo, Y., and Son, K., Standardization and computer programing of safety factors of corrugated fiberboard containers for agricultural products (I) – Physical properties of corrugated fiberboard and estimation of box compressive strength with changes of relative humidity -, Proceedings from Korea TAPPI spring conference (2005)

Johansson, L-S., Tammelin, T., Campbell, J M., Setälä, H., and Ö sterberg, M., Experimental evidence on medium driven cellulose surface adaptation demonstrated using nanofibrillated cellulose, Soft Matter, 7(22):10917-10924 (2011)

Johnson, R. K., Zink-Sharp, A., Renneckar, S. H., and Glasser, W. G., A new bio-based nanocomposite: Fibrillated TEMPO-oxidized cellulose in hydroxypropylcellulose matrix, Cellulose 16(2):227-238 (2008)

Jonoobi, M., Harun, J., Mathew, A., Hussein, M., and Oksman, K., Preparation of cellulose nanofibers with hydrophobic surface characteristics. Cellulose 17(2):299–307 (2010)

Kang, K., and Kim, H., Effects of temperature and relative humidity on the physical properties of electronic copying paper, Journal of Korea TAPPI, 44(3):70-78 (2012)

Karnitz Jr. O., L.V.A. Gurgel, J.C.P.Melo, V.R. Botaro, T.M.S. Melo, R.P.F. Gil, L.F. Gil, Adsorption of heavymetal ion fromaqueous singlemetal solution by chemically modified sugarcane bagasse, Bioresour. Technol. 98:1291–1297 (2007)

Kettunen, M., Silvennoinen, R. J., Houbenov, N., Nykänen, A., Ruokolainen, J., Sainio, J., Pore, V., Kemell, M., Ankerfors, M., Lindström, T., Ritala, M., Ras, R. H. A., and Ikkala, O., Photoswitchable superabsorbency based on nanocellulose aerogels, Adv, Funct. Mater. 21(3):510-517 (2011)

Khalil, M. L., Beliakova, M. K., and Aly, A. A., Preparation of some starch ethers using the semi-dry state process. Carbohydrate Polymers, 46(3):217–226 (2001)

Kistler, S., Coherent expanded aerogels and jellies, Nature 127:741-741 (1931)

Kim, H., Choi, W., and Um, G., The effect of atmospheric conditions on the physical and mechanical properties of linerboard, Journal of Korea TAPPI, 38(5):60-65 (2006)

Kolakovic, R., Peltonen, L., Laaksonen, T., Putkisto, K., Laukkanen, A., and Hirvonen, J., Spray-dried cellulose nanofi bers as novel tablet excipient. AAPS PharmSciTech 12(4):1366-1373 (2011).

Koga, H., Azetsu, A., Tokunaga, E., Saito, T., Isogai, A., and Kitaoka, T., Topological loading of Cu(I) catalysts onto crystalline cellulose nanofibrils for the Huisgen click reaction, J. Mater. Chem. 22(12):5538-5542 (2012)

Korhonen, J. T., Kettunen, M., Ras, R. H. A., and Ikkala, O., Hydrophobic nanocellulose aerogels as floating, sustainable, reusable, and recyclable oil absorbents, ACS Appl. Mater. Interfaces, 3(6):1813-1816 (2011)

Lee, M., Jo, J., and Shin, J., Changes of the physical properties of corrugated fiberboard boxes for fruit and vegetable packaging by preservation temperature and relative humidity, Journal of Korea TAPPI 34(1):46-53 (2002)

Li, S., Xiao, M., Zheng, A., and Xiao, H., Cellulose microfibrils grafted with PBA via surface initiated atom transfer radical polymerization for biocomposite reinforcement, Biomacromolecules 12(9):3305-3312 (2011)

Liebner, F., Potthas, A., Rosenau, T., Haimer, E., and Wendland, M., Cellulose aerogels: Highly porous, ultra-lightweight materials, Holzforschung 62(2):129-135 (2008)

Liebner, F., Haimer, E., Wendland, M., Neouze, M., Schulfter, K., Miethe, P., Henze, T., Potthast, A., and Rosenau, T., Aerogels from unaltered bacterial cellulose: application of scCO2 drying for the preparation of shaped, ultra-lightweight cellulosic aerogels, Macromol. Biosci. 10(4):345-352 (2010)

Littunen, K., Hippi, U., Johansson, L. S., Ö sterberg, M., Tammelin, T., Laine, J., and Seppälä, J., Free radical graft copolymerization of nanofibrillated cellulose with acrylic monomers. Carbohydr. Polym. 84(3):1039–1047 (2011)

Liu, A., Walther, A., Ikkala, O., Belova, L., and Berglund, L. A. Clay nanopaper with tough cellulose nanofiber matrix for fire retardancy and gas barrier functions Biomacromolecules, 12(3):633–641 (2011)

Lönnberg, H., Larsson, K., Lindström, T., Hult, A., and Malmström, E., Synthesis of polycaprolactone-grafted microfibrillated cellulose for use in novel bionanocomposites--influence of the graft length on the mechanical properties, ACS Appl. Mater. Interfaces 3(5):1426-1433 (2011)

Lu, J., Askeland, P., and Drzal, L.T., Surface modification of microfibrillated cellulose for epoxy composite applications, Polymer 49(5):1285-1296 (2008)

Lu, X., Arduinischuster, M. C., Kuhn, J., Nilsson, O., Fricke, J., and Pekala, R. W., Thermal conductivity of monolithic organic aerogels, Science 255(5047):971-972 (1992)

Missoum, K., Belgacem, M. N., and Bras, J., Nanofibrillated cellulose surface modification: A review materials, 6(5):1745-1766 (2013)

Nachtergaele, W., The Benefits of Cationic Starches for the Paper Industry, Starch – Stärke, 41(1):27-31 (1989)

Nakagaito, A. N. and Yano, H., The effect of morphological changes from pulp fiber towards nano-scale fibrillated cellulose on the mechanical properties of high-strength plant fiber based composites, Appl. Phys. A 78(4):547-552 (2004)

Olsson, R. T., Azizi Samir, M. A. S., Salazar-Alvarez, G., Belova, L., Ström, V., Berglund, L. A., Ikkala, O., Nogués, J., and Gedde, U. W, Making flexible magnetic aerogels and stiff magnetic nanopaper using cellulose nanofibrils as templates, Nature Nanotechnology, 5:584-588 (2010)

Pääkkö, M., Ankerfors, M., Kosonen, H., Nykänen, A., Ahola, S., and Ö sterberg, M., Enzymatic hydrolysis combined with mechanical shearing and high-pressure homogenization for nanoscale cellulose fibrils and strong gels, Biomacromolecules 8(6):1934-1941 (2007)

Pääkkö, M., Vapaavuori, J., Silvennoinen, R., Kosonen, H.,. Ankerfors, M., Lindström, T., Berglund, L. A., and Ikkala, O., Long and entangled native cellulose I nanofibers allow flexible aerogels and hierarchically porous templates for functionalities, Soft Matter 4(12):2492-2499 (2008)

Pekala, R.W., Organic aerogels from the polycondensation of resorcinol with formaldehyde, J. Mater. Sci. 24(9):3221–3227 (1989)

Qi, H., Mäder, E., and Liu, J., Electrically conductive aerogels composed of cellulose and carbon nanotubes, J. Mater. Chem. A 1(34):9714-9720 (2013)

Rodionova, G, Lenes, M., Eriksen, Ø ., Hoff, B. H., and Gregersen, Ø ., Surface modification of microfibrillated cellulose films by gas-phase esterification: Improvement of barrier properties, Proceedings of 2010 TAPPI International conference on nanotechnology for the forest product industry, Finland, 27-29 (2010)

Russler, A., Wieland, M., Bacher, M., Henniges, U., Miethe, P., Liebner F., Potthast, A., and Rosenau, T., AKD-Modification of bacterial cellulose aerogels in supercritical CO2, Cellulose 19(4):1337-1349 (2012)

Ryu, J., Youn, H. J., Sim, K., and Lee, H., Network strength and structure of nanofibrillated cellulose suspension with PEI adsorption, Proceeding of 2012 spring conference of the KTAPPI, Seoul, 79-86 (2012)

Saito, T., and Isogai, A., TEMPO-mediated oxidation of native cellulose. The effect of oxidation conditions on chemical and crystal structures of the water-insoluble fraction, Biomacromolecules 5(5):1983-1989 (2004)

Saito, T., Nishiyama, Y., Putaux, J., Vignon, M., and Isogai, A., Homogeneous suspensions of individualized microfibrils from TEMPO-catalyzed oxidation of native cellulose, Biomacromolecules 7(6):1687-1691 (2006)

Saito, T., Kimura, S., Nishiyama, Y., and Isogai, A., Cellulose nanofibers prepared by TEMPO-mediated oxidation of native cellulose, Biomacromolecules 8(8):2485-2491 (2007)

Saito, T., Hirota, M., Tamura, N., Kimura, S., Fukuzumi, H., and Heux, L., Individualization of nano-sized plant cellulose fibrils by direct surface carboxylation using TEMPO catalyst under neutral condistion, Biomacromolecules 10(7):1992-1996 (2009)

Sakurada, I., Nukushina, Y., and Ito, T., Experimental determination of the elastic modulus of crystalline regions in oriented polymers. Journal of Polymer Science, 57(165):651–660 (1962)

Salmén, Vasquez, V.R., Coronella, C.J., A simple model for vapor-moisture equilibrium in biomass substrates. AIChE Journal 55:1595–1603 (2009)

Sehaqui, H., Salajková, M., Zhou, Q., and Berglund, L. A., Mechanical performance tailoring of tough ultra-high porosity foams prepared from cellulose I nanofiber suspensions, Soft Matter 6(8):1824-1832 (2010)

Siqueira, G., Bras, J., and Dufresne, A., Luffa cylindrical as a lignocellulosic source of fiber, microfibrillated cellulose and cellulose nanocrystals, Bioresources 5(2):727-740 (2010)

Sehaqui, H., Zhou, Q., and Berglund, L. A., High-porosity aerogels of high specific surface area prepared from nanofibrillated cellulose (NFC), Composites Science and Technology 71(13):1593-1599 (2011)

Shin, H., The effect of cellulose crystallinity and oxidized starch as surface sizing on permanence of paper, Master of Science thesis, Seoul national university (2011)

Siqueira, G., Tapin-Lingua, S., Bras, J., Da Silva Perez, d., and Dufresne, A., Morphological investigation of nanoparticles obtained from combined mechanical shearing, and enzymatic and acid hydrolysis of sisal fibers, Cellulose 17(6):1147-1158 (2010a),

Siqueira, G., Tapin-Lingua, S., Bras, J., Da Silva Perez, d., and Dufresne, A., Mechanical properties of natural rubber nanocomposites reinforced with cellulosic nanoparticles obtained from combined mechanical shearing, and enzymatic and acid hydrolysis of sisal fibers, Cellulose 18(1):57-65 (2011b)

Song, D., Kim, C., Jung, H., Lee, Y., Kim, J., Kim, G., and Park, C., Physical properties of shock-absoring materials made of pulp fibers for packaging, Journal of Korea TAPPI 37(3):41-49 (2005)

Svagan, A. J., Azizi Samir, M. A. S., and Berglund, L. A., Biomimetic foams of high mechanical performance based on nanostructured cell walls reinforced by native cellulose nanofibrils, Adv. Mater. 20(7):1263-1269 (2008)

Syverud, K. and Stenius, P., Strength and barrier properties of MFC films, Cellulose 16(1):75-85 (2009)

Syverud, K., Xhanari, K., Chinga-Carrasco, G., Yu, Y., and Stenius, P., Films made of cellulose nanofibrils: surface modification by adsorption of a cationic surfactant and characterization by computer-assisted electron microscopy, J. Nanopart. Res. 13(2):773-782 (2011)

Tan, C., Fung, B. M., Newman, J. K., and Vu, C., Organic aerogels with very high impact strength, Adv. Mater. 13(9):644-646 (2001)

Taipale, T., Ö sterberg, M., Nykänen, A., Ruokolainen, J., and Lainen, J., Effect of microfibrillated cellulose and fines on the drainage of kraft pulp suspension and paper strength, Cellulose 17(5):1005-1020 (2010)

Taiguchi, T., and Okamura, K., New films produced from nicrofibrillated natural fibres, polym. int. 47(3):291-294 (1988)

Tingaut, P., Zimmermann, T., and Lopez-Suevos, F., Synthesis and characterization of bionanocomposites with tunable properties from poly(lactic acid) and acetylated microfibrillated cellulose, Biomacromolecules 11(2):454-464 (2010)

Turbak, A. F., Synder, F. W., and Sandberg, K. R., Microfibrillated cellulose, a new cellulose product: properties, uses, and commercial potential, J. Appl. Polym. Sci. Appl. Polym. Symp. 37:815-527 (1983)

Uetani, K., and Yano, H., Nanofibrillation of wood pulp using a high-speed blender, Biomacromolecules 12(2):348-353 (2011)

Valo, H., Arola, S., Laaksonen, P., Torkkeli, M., Peltonen, L., and Linder, M. B., Drug release from nanoparticles embedded in four different nanofibrillar cellulose aerogels. European Journal of Pharmaceutical Sciences. 50:69-77 (2013)

Wågberg, L., Decher, G., Norgren, M., Lindström, T., Ankerfors, M., and Axnäs, K., The build-up of polyelectrolyte multilayers of microfibrillated cellulose and cationic polyelerolytes, Langmuir 24(3):784-795 (2008)

Wang, Q. Q., Zhu, J. Y., Reiner, R. S., Verrill, S. P, Baxa, U., and McNeil, S. E., Approaching zero cellulose loss in cellulose nanocrystal (CNC) production: recovery and characterization of cellulosic solid residues (CSR) and CNC, Cellulose 19(6):2033-2047 (2012)

Wang, Y., Cellulose fiber dissolution in sodium hydroxide solution at low temperature: dissolution kinetics and solubility improvement, Ph. D. thesis, Georgia Institute of Technology, (2008)

Wang, Y. Y., Tian, M., Xu, H. X., and Fan, P., Influence of moisture on mechanical properties of cellulose insulation paper, Int. J. Mod. Phys. B 28(7):1450051-1-1450051-12 (2014)

Xhanari, K., Syverud, K., Chinga-Carrasco, G., Paso, K., and Stenius, P., Reduction of water wettability of nanofibrillated cellulose by adsorption of cationic surfactants, Cellulose 18(2):257-270 (2011)

Yano, H., and Nakahara, S., Bio-composites produced from plant microfiber bundles with a nanometer unit web-like network, J. Mater. Sci. 39(95):1635–1638 (2004)

Yang, C. Q., Chen, D., Guan, J., and He, Q., Cross-linking cotton cellulose by the combination of maleic acid and sodium hypophosphite. 1. Fabric wrinkle resistance, Ind. Eng. Chem. Res. 49:8325-8332 (2010)

Zaman, M., Xiao, H., Chibante, F., and Ni, Y., Synthesis and characterization of cationically modified nanocrystalline cellulose, Carbo. Polym. 89:163-170 (2012)

Zimmermann, T., Bordeanu, N., and Strub, E., Properties of nanofibrillated cellulose from different raw materials and its reinforcement potential, Carbohyd. Polym. 79(4):1086-1093 (2010)

Zhang, W., Yaan, Z., Canhui, L., and Yulin, D., Aerogels from crosslinked cellulose nano/micro-fibrils and their fast shape recovery property in water, J. Mater. Chem. 22(23):11642-11650 (2012)

Zhao, B., and Brittain, W. J., Polymer brushes: surface-Immobilized macromolecules, Prog. Polym. Sci. 25(5):677-710 (2000)

Zheng, Q., Cai, Z., and Gong, S., Green synthesis of polyvinyl alcohol (PVA)-cellulose nanofibril (CNF) hybrid aerogels and their use as superabsorbents, J. Mater. Chem. A 2(9):3110-3118 (2014)

초 록

말레인산과 차아인산나트륨을 이용해 가교 결합된 셀룰로오스 나노피브릴 에어로젤의 제조 및 특성 연구

서울대학교 대학원
산림과학부
환경재료과학전공
김채훈

셀룰로오스 나노피브릴은 셀룰로오스 섬유에 기계적인 전단력을 가해 얻어지는 두께 5 – 50 nm, 길이 수 마이크로 미터의 섬유상의 나노 물질이다. 셀룰로오스 나노피브릴은 학계와 산업계로부터 다양한 응용분야로 연구되어왔으며, 특히 에어로젤 소재로 적용이 유리한 특성을 가진다. 셀룰로오스 나노피브릴은 1 %의 매우 낮은 농도의 서스펜션 상태에서도 기계적인 엉킴에 의해 하이드로젤 구조를 형성하는 특징이 있다. 이러한 하이드로젤을 동결건조 처리시킴으로써 비교적 간단하고 경제적인 방법으로 에어로젤을 제조할 수 있다. 한편, 셀룰로오스 나노피브릴 에어로젤은 수소 결합을 통해 네트워크 구조를 형성하고 있어 물에 접촉하게 되면 그 구조가 쉽게 파괴되는 특징이 있다. 이러한 문제로 인해 셀룰로오스 나노피브릴 에어로젤은 광범위한 응용에 제약이 있다.

본 연구에서는 가교 결합된 셀룰로오스 나노피브릴 에어로젤을 제조하였다. 가교 결합 처리제로 말레인산과 차아인산나트륨을 사용하였다. 가교 결합 처리 과정은 에스테르화 반응을 통한 셀룰로오스 나노피브릴 표면으로의 말레인산 도입 공정과 도입된 말레인 산 사이에 차아인산에 의한 가교결합이 형성되는 공정으로 이루어져 있다. 이러한 방법으로 제조한 가교 결합된 에어로젤은 기존 셀룰로오스 나노피브릴 에어로젤과 달리 물에 대한 저항성이 강화되어 물 속에서 일정 수준의 전단력이 가해져도 에어로젤의 구조를 유지하는 특성을 나타내었으며, 물을 흡수하는 특성을 나타내었다. 또한 물에 젖은 상태에서 외력에 의해 압축된 후 외력이 제거되면 원래의 형상을 빠르게 회복하는 특성을 나타내었다.

가교 결합된 셀룰로오스 나노피브릴 에어로젤은 약물 담체, 약품 지지체 등의 의약 분야로의 적용 가능성이 제시되었다. 따라서 이러한 응용 과정에 있어서 요구되는 이온 흡착 특성을 고찰하였다. 이를 위해 양이온성, 음이온성의 금속 이온이 모델 물질로서 사용되었다. 가교 결합된 셀룰로오스 나노피브릴 에어로젤의 표면 전하를 양성으로 개질하기 위해 glycidy−ltrimethylammonium chloride (GTMAC)의 에테르화 반응을 이용하여 셀룰로오스 나노피브릴을 양성으로 개질하였다. 그 결과 양성 셀룰로오스 나노피브릴의 제타 전위가 최대 +39.5 mV를 나타내었다. 이를 통해 제조된 가교 결합된 양성 셀룰로오스 나노피브릴 에어로젤은 전하를 나타내는 작용기로 사차암모늄기와 카르복실기를 갖고

있었다. 한편 가교 결합된 음성 셀룰로오스 나노피브릴 에어로젤은 카르복실기를 갖고 있었다. 따라서 가교 결합된 셀룰로오스 나노피브릴 에어로젤은 pH에 의해 표면 전하 특성이 영향받았으며 그에 따라 이온의 흡착성능도 영향받았다. 가교 결합된 셀룰로오스 나노피브릴 에어로젤의 최대 이온 흡착 용량을 평가하기 위해 Langmuir model에 의거하여 흡착 등온선을 도출하였다. 그 결과 가교 결합된 음성 셀룰로오스 나노피브릴 에어로젤은 Ni^{2+} 이온에 대하여 0.79 mmol/g, 가교 결합된 양성 셀룰로오스 나노피브릴 에어로젤은 MnO_4^- 이온에 대하여 0.62 mmol/g의 최대 이온 흡착 용량을 나타내었다. 이러한 성능은 기존 연구에서 보고된 셀룰로오스 개질체의 최대 이온 흡착 용량에 비해서는 낮은 수준이었으나 기존 상용 이온 교환 수지에 비해서는 매우 높은 수준으로 평가되었다.

주요어 : 셀룰로오스 나노피브릴, 에어로젤, 가교결합, shape recovery, 양성 개질, 이온 흡착

학번 : 2008-21294